Synthesis, Structural Evaluation, and Estrogen Receptor Interaction of 2,3-Diarylpiperazines

Ronald Gust,* Roland Keilitz, and Kathrin Schmidt

Institute of Pharmacy, Free University of Berlin, Königin-Luise Strasse 2+4, D-14195 Berlin, Germany

Received January 29, 2002

To develop novel estrogen receptor (ER) ligands, ring-fused derivatives of the hormonally active (1*R*,2*S*)/(1*S*,2*R*)-1-(2-chloro-4-hydroxyphenyl)-2-(2,6-dichloro-4-hydroxyphenyl)ethylenediamine **4b** were synthesized. (2*R*,3*S*)/(2*S*,3*R*)-2-(2-Chloro-4-hydroxyphenyl)-3-(2,6-dichloro-4-hydroxyphenyl)piperazine **4** induced ligand-dependent gene expression in MCF-7-2a cells, stably transfected with the plasmid ERE_{wtc}luc and was therefore used as a lead structure. The influence of the substitution pattern in the aromatic rings (4-OH (**1**), 2-F,4-OH (**2**), 2-Cl,4-OH (**3**), 2,6-Cl_2,3-OH (**5**), and 2,6-Cl_2,4-OH (**6**)) and the effect of *N*-ethyl chains on the ER binding and activation of gene expression were studied. The synthesis started from the respective methoxy-substituted (1*R*,2*S*)/(1*S*,2*R*)-configurated 1,2-diarylethylenediamines **6b** to **4b**, which were reacted with dimethyl oxalate in order to get 5,6-diarylpiperazine-2,3-diones. Reduction with BH_3·tetrahydrofuran and ether cleavage with BBr_3 yielded the piperazines **1**−**6**. The *N*-alkylation of the piperazines **1a**−**3a**, which was employed for obtaining compounds **7**−**11**, was succeeded by acetic anhydride followed by reduction and ether cleavage. Nuclear magnetic resonance (NMR) spectroscopical studies revealed a synclinal conformation of the 1,2-diarylethane pharmacophore and a preference of the substituents at the heterocyclic ring for an equatorial position. This spatial structure prevents an interaction with the ER analogously to that of estradiol (**E2**). Therefore, the piperazines can displace **E2** from its binding site only to a very small extent. Only the *N*-ethyl (**8**) and *N*,*N*′-diethyl (**11**) derivatives of piperazine **3** showed relative binding affinity values > 0.1% (**8**, 0.42%, and **11**, 0.17%). Nevertheless, ER-mediated gene activation was verified for the piperazines **4** (20%), **6** (73%), **7** (34%), **8** (74%), and **11** (37%) (concentration, 1 μM; **E2**, 100% activation) on the MCF-7-2a cell line. O-methylation led to completely inactive compounds and showed the necessity of H bridges from the piperazines to the ER for activating gene expression.

Introduction

Estrogen Receptor (ER). Two forms have been described (α and β). In the present paper, we refer solely to ERα, since it is verified that this receptor is mainly present in MCF-7 mammary carcinoma cells. A member of the steroid receptor gene family acts as a transcriptional factor, which is involved in the regulation of diverse arrays of target genes.[1] To activate the ER, a ligand-dependent conformational change of the receptor molecule is necessary. The expression of target genes takes place after the dimerization of drug−receptor complexes and binding to the estrogen response elements (ERE) at the DNA.[2]

The drugs show an agonistic, antagonistic, or a tissue selective mixed agonistic/antagonistic profile depending on their structure.[3] Such compounds, called selective estrogen receptor modulators (SERMs),[4] are of great interest in cancer chemotherapy and estrogen replacement therapy in postmenopausal women.[5,6] SERMs inhibit bone resorption, can prevent osteoporosis,[7] and cause beneficial effects on the cardiovascular system[8] and the central nervous system.[9] Furthermore, estrogen exposure is associated with a decrease of coronary heart disease, improvements in cognitive function, and a delay in the onset of Alzheimer's disease.

Despite its high benefit, the long-term treatment with SERMs is often limited due to intolerable side effects, for example, benign and malignant lesion of the uterus. Therefore, the search for new SERMs among both existing and new drugs has been a challenging task in recent years.[10]

Several research groups performed modifications at the 7α- and 11β-position with the aim to change the hormonal profile of **E2** from estrogen to antiestrogen.[11,12] Fulvestrant (faslodex) is a 7α-alkylamide of **E2** and as pure antiestrogen already used in clinical trials.[13] Further investigations focused on the design of drugs with high selectivity for one of the ER subtypes, using 1,3,5-triaryl-4-alkylpyrazoles[14] or 2-amino-4,6-diarylpyridines[15] as lead structures.

Our investigations show that not only flat but also puckered molecules interact with the ER and activate ligand-dependent gene expression in MCF-7-2a breast cancer cells, stably transfected with the plasmid ERE_{wtc}luc.[16] The (2*R*,3*S*)/(2*S*,3*R*)-2-(2-chloro-4-hydroxyphenyl)-3-(2,6-dichloro-4-hydroxyphenyl)piperazine **4**, a ring-fused derivative of the hormonally active (1*R*,2*S*)/(1*S*,2*R*)-1-(2-chloro-4-hydroxyphenyl)-2-(2,6-dichloro-4-hydroxyphenyl)ethylenediamine, activated expression of

* To whom correspondence should be addressed. Tel.: (030)838 53272. Fax: (030)838 56906. E-mail: rgust@zedat.fu-berlin.de.

10.1021/jm0208368 CCC: $22.00
Published on Web 04/25/2002

Chart 1. Structural Formulas of Compounds Referred to in the Text

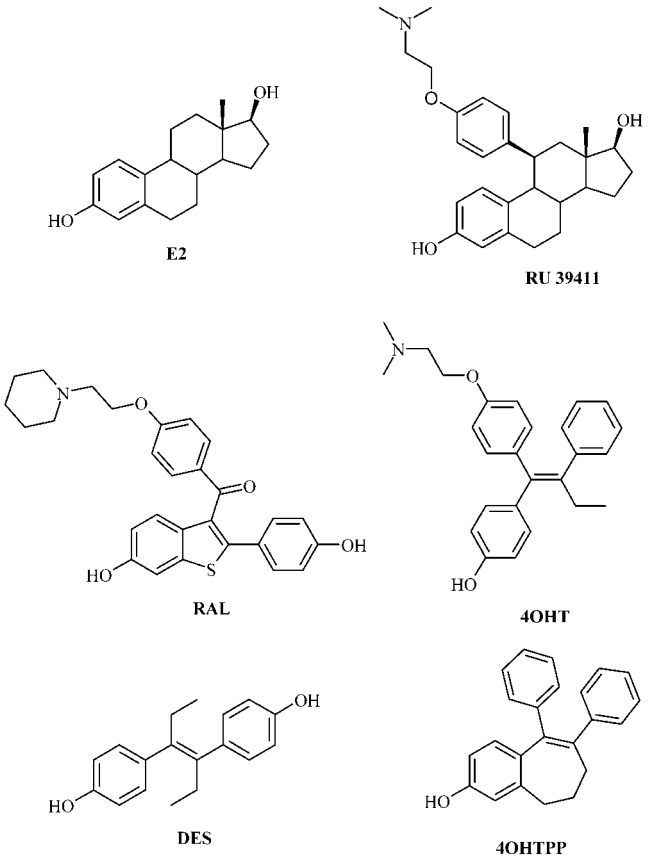

the luciferase gene in MCF-7-2a cells. In contrast, **4** was not able to displace **E2** from its binding site at the ER in the competition experiment with [^{3}H]**E2** using calf uterine cytosol (relative binding affinity (RBA) < 0.02%). This is the consequence of a synclinal arrangement of the 1,2-diarylethane moiety already identified as an essential pharmacophore.[17] This spatial structure is quite different from those of steroidal or nonsteroidal estrogens such as diethylstilbestrol (DES) and **E2** (see Chart 1). Therefore, a different binding mode at the ER is assumed. In this paper, experiments to optimize the ER-mediated effects of 2,3-diarylpiperazines by variation of the substitution pattern in the aromatic rings and by *N*-alkylation are described.

Results

Synthesis. The synthesis of the piperazines was performed in a two step reaction according to Scheme 1. Heating of the respective 1,2-diarylethylenediamines **1b**−**6b**[18−20] together with dimethyl oxalate in dioxane under reflux yielded in the first reaction step the piperazine-2,3-diones, which were reduced to the 2,3-diarylpiperazines **1a**−**6a**. For *N*-alkylation, the 2,3-bis-(4-methoxyphenyl)piperazines **1a**−**3a** were reacted with acetic anhydride and subsequently reduced with BH_3·tetrahydrofuran (THF) (Scheme 2).

In the case of the *N*,*N*′-diethyl-2,3-diarylpiperazines **10a** and **11a**, the reduction led to a partial cleavage of one of the N-standing ethyl groups, so that the *N*-ethyl-2,3-diarylpiperazines **7a** and **8a** could be isolated, too. The hydroxy-substituted piperazines **1**−**11** were finally generated by ether cleavage with BBr_3 (Scheme 3).

Scheme 1. Synthesis of the 2,3-Diarylpiperazines **1a**−**6a**

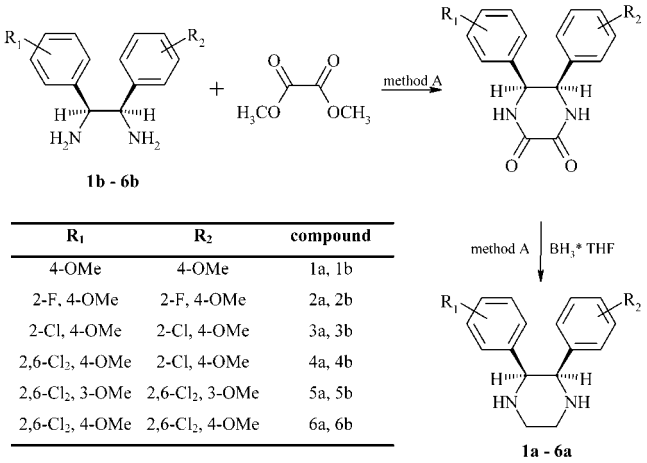

R_1	R_2	compound
4-OMe	4-OMe	1a, 1b
2-F, 4-OMe	2-F, 4-OMe	2a, 2b
2-Cl, 4-OMe	2-Cl, 4-OMe	3a, 3b
2,6-Cl_2, 4-OMe	2-Cl, 4-OMe	4a, 4b
2,6-Cl_2, 3-OMe	2,6-Cl_2, 3-OMe	5a, 5b
2,6-Cl_2, 4-OMe	2,6-Cl_2, 4-OMe	6a, 6b

Scheme 2. *N*-Alkylation of the 2,3-Diarylpiperazines **1a**−**3a**

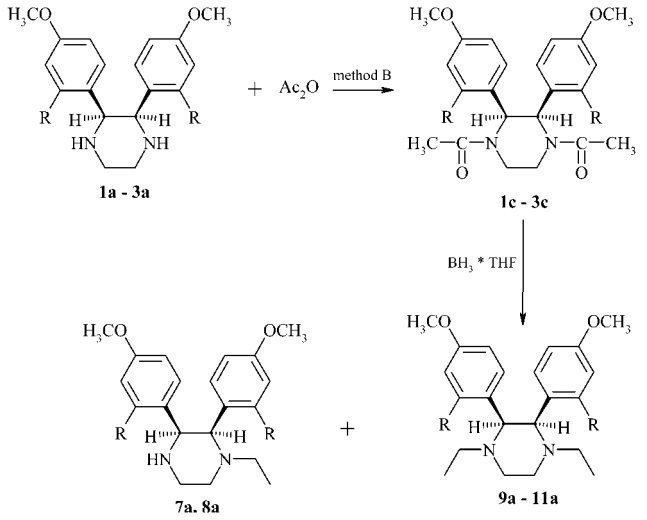

R	compound
H	1a, 1c, 9a
F	2a, 2c, 7a, 10a
Cl	3a, 3c, 8a, 11a

Structural Evaluation. In solution, the piperazine ring undergoes a dynamic interconversion between two limiting structures (see Figure 1). Because it is well-known that substituents influence the dynamic effects of five- and six-membered rings,[21,22] we studied the conformeric behavior of the heterocycles **1**−**11** using ^{1}H nuclear magnetic resonance (NMR) and molecular modeling methods.

The (2*R*,3*S*)/(2*S*,3*R*) configuration forces the phenyl rings at the piperazine ring in synclinal position (see Figure 1). In both limiting structures, one of the phenyl rings is axially standing and the methine protons (H1a and H1b) as well as the methylene protons (H2a and H2b) are nonequivalent. During the interconversion, the molecule becomes symmetric (presumption: Ar = Ar′), and in the ^{1}H NMR spectra, the diastereotopic split of the resonances is lost.

The spectra of the piperazines **1**−**3**, **5**, and **6** show only a singlet resonance for H1a/H1b and two signal

Table 1. NMR Data[a] of 2,3-Diarylpiperazines

compd	methine H1a,H1b	methylene H2a,H2b	aromatic H	*N*-ethyl	OH
1	3.99 (s, 2H)	2.64−2.71 (m, 2H) 2.97−3.04 (m, 2H)	6.49 (AA′*BB*′, 4H) 7.19 (*AA*′BB′, 4H)		9.00 (s, 2H)
2	4.35 (s, 2H)	2.66−2.74 (m, 2H) 2.97−3.05 (m, 2H)	6.33 (dd, $^3J_{(H,F)}$ = 12.5 Hz, ^4J = 1.9 Hz, 2H) 6.38 (dd, ^3J = 8.6 Hz, ^4J = 1.9 Hz, 2H) 7.67 (dd, ^3J = 8.6 Hz, $^4J_{(H,F)}$ = 8.8 Hz, 2H)		9.51 (s, 2H)
3	4.57 (s, 2H)	2.66−2.78 (m, 2H) 2.95−3.07 (m, 2H)	6.53 (dd, ^3J = 8.6 Hz, ^4J = 2.1 Hz, 2H) 6.62 (d, ^4J = 2.1 Hz, 2H) 7.85 (d, ^3J = 8.6 Hz, 2H)		9.55 (s, 2H)
4	4.82 (d, ^3J = 4.9 Hz, 1H) 5.02 (d, ^3J = 4.9 Hz, 1H)	2.84−2.91 (m, 1H) 3.00−3.12 (m, 1H) 3.28−3.42 (m, 1H) 3.54−3.66 (m, 1H)	6.58 (d, ^4J = 2.6 Hz, 1H) 6.62 (s, 2H) 6.74 (dd, ^3J = 8.7 Hz, ^4J = 2.6 Hz, 1H) 8.10 (d, ^3J = 8.7 Hz, 1H)		
5	5.37 (s, br, 2H)	2.96−3.13 (m, 2H) 3.26−3.43 (m, 2H)	6.73 (d, ^3J = 8.8 Hz, 2H) 7.00 (d, br, ^3J = 8.8 Hz, 2H)		
6	5.20 (s, 2H)	2.96−3.09 (m, 2H) 3.34−3.48 (m, 2H)	6.65 (s, 4H)		
7	4.26 (d, ^3J = 3.8 Hz, 1H) 4.37 (d, ^3J = 3.8 Hz, 1H)	2.47−2.52 (m, 1H) 2.65−2.75 (m, 1H) 2.93−3.00 (m, 1H) 3.14−3.21 (m, 1H)	6.24 (dd, $^3J_{(H,F)}$ = 12.3 Hz, ^4J = 2.4 Hz, 1H) 6.27 (dd, ^3J = 8.6 Hz, ^4J = 2.4 Hz, 1H) 6.37 (dd, $^3J_{(H,F)}$ = 12.4 Hz, ^4J = 2.4 Hz, 1H) 6.94 (dd, ^3J = 8.6 Hz, ^4J = 2.4 Hz, 1H) 7.08 (dd, ^3J = 8.6 Hz, $^4J_{(H,F)}$ = 8.6 Hz, 1H) 8.09 (dd, ^3J = 8.6 Hz, $^4J_{(H,F)}$ = 8.7 Hz, 1H)	0.95 (t, ^3J = 7.1 Hz, 3H) 2.00−2.09 (m, 1H) 2.19−2.28 (m, 1H)	9.51 (s, 2H)
8	4.46 (d, ^3J = 3.8 Hz, 1H) 4.62 (d, ^3J = 3.8 Hz, 1H)	2.52−2.60 (m, 1H) 2.82−2.90 (m, 1H) 2.90−3.00 (m, 1H) 3.14−3.22 (m, 1H)	6.37 (dd, ^3J = 8.6 Hz, ^4J = 2.3 Hz, 1H) 6.52 (d, ^4J = 2.3 Hz, 1H, Ar*H*-3) 6.60 (dd, ^3J = 8.6 Hz, ^4J = 2.3 Hz, 1H) 6.64 (d, ^4J = 2.3 Hz, 1H) 6.96 (d, ^3J = 8.6 Hz, 1H) 8.15 (d, ^3J = 8.6 Hz, 1H);	0.94 (t, ^3J = 7.1 Hz, 3H) 2.03−2.12 (m, 1H) 2.28−2.38 (m, 1H)	9.52 (s, 2H)
9	3.57 (s, 2H)	2.34−2.50 (m, 2H) 2.98 (br, 2H)	6.47 (AA′*BB*′, 4H) 7.00 (*AA*′BB′, 2H)	0.93 (t, ^3J = 7.1 Hz, 6H) 1.90−2.02 (m, br, 2H) 2.22 (br, 2H)	9.04 (s, 2H)
10	4.07 (s, 2H)	2.51 (covered by solvent peak); 3.02 (br, 2H)	6.33 (d, br, $^3J_{(H,F)}$ = 12.5 Hz, 2H) 6.38 (d, br, ^3J = 8.1 Hz, 2H) 7.37 (br, 2H)	0.96 (t, ^3J = 6.8, 6H) 2.02 (br, 2H) 2.30 (br, 2H)	9.59 (s, 2H)
11	4.33 (s, 2H)	2.49−2.58 (m, 2H) 3.05−3.14 (m, 2H)	6.49 (dd, ^3J = 8.6 Hz, ^4J = 2.2 Hz, 2H) 6.59 (d, ^4J = 2.2 Hz, 2H) 7.39 (br, 2H)	0.94 (t, ^3J = 7.1 Hz, 6H) 2.07−2.16 (m, 2H) 2.17−2.27 (m, 2H)	9.57 (s, 2H)

[a] 400 MHz spectra in [D$_6$]DMSO (**1**−**3** and **7**−**11**), [D$_4$]methanol (**4**−**6**), with TMS as internal standard; δ(TMS) = 0. Representation of the chemical shifting (δ) in ppm.

Scheme 3. Ether Cleavage of the Piperazines **1a**−**11a** with BBr_3

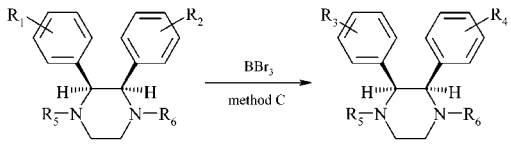

1a - 11a **1 - 11**

R_1	R_2	R_3	R_4	R_5	R_6	compound
4-OMe	4-OMe	4-OH	4-OH	H	H	1a, 1
2-F, 4-OMe	2-F, 4-OMe	2-F, 4-OH	2-F, 4-OH	H	H	2a, 2
2-Cl, 4-OMe	2-Cl, 4-OMe	2-Cl, 4-OH	2-Cl, 4-OH	H	H	3a, 3
2,6-Cl_2, 4-OMe	2,6-Cl_2, 4-OMe	2,6-Cl_2, 4-OH	2-Cl, 4-OH	H	H	4a, 4
2,6-Cl_2, 3-OMe	2,6-Cl_2, 3-OMe	2,6-Cl_2, 3-OH	2,6-Cl_2, 3-OH	H	H	5a, 5
2,6-Cl_2, 4-OMe	2,6-Cl_2, 4-OMe	2,6-Cl_2, 4-OH	2,6-Cl_2, 4-OH	H	H	6a, 6
2-F, 4-OMe	2-F, 4-OMe	2-F, 4-OH	2-F, 4-OH	Ethyl	H	7a, 7
2-Cl, 4-OMe	2-Cl, 4-OMe	2-Cl, 4-OH	2-Cl, 4-OH	Ethyl	H	8a, 8
4-OMe	4-OMe	4-OH	4-OH	Ethyl	Ethyl	9a, 9
2-F, 4-OMe	2-F, 4-OMe	2-F, 4-OH	2-F, 4-OH	Ethyl	Ethyl	10a, 10
2-Cl, 4-OMe	2-Cl, 4-OMe	2-Cl, 4-OH	2-Cl, 4-OH	Ethyl	Ethyl	11a, 11

groups for H2a and H2b (Table 1) indicating an interconversion of the piperazine ring (conformations I and II; see Figure 1).

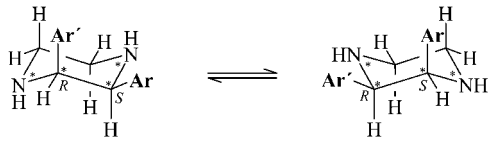

Figure 1. Arrangement of the aryl residues during the conversion of the piperazine ring.

In the spectra of (2*R*,3*S*)/(2*S*,3*R*)-2-(2-chloro-4-hydroxyphenyl)-3-(2,6-dichloro-4-hydroxyphenyl)piperazine **4**, these signal groups are split due to the asymmetric character of the molecule. The coupling constant $^3J_{H1a-H1b}$ = 4.9 Hz follows the Karplus dependence[23] and correlates with an angle of 35−55°. This value can only be realized if the piperazine ring adapts a relatively stable conformation without interconversion. Analogously to related [1,2-diarylethylenediamine]platinum(II) complexes,[18,24] a conformation is assumed in which the 2,6-dichloro-4-hydroxyphenyl ring is preferably equatorially arranged and the 2-chloro-4-hydroxyphenyl ring is axially arranged (see Figure 1).

These structures were refined by molecular modeling methods using Tripos Sybyl 6.6 (Tripos Force Field,

Table 2. NMR Data[a] of COSY, NOE, and NOESY Experiments with Piperazine **7**

chemical shift (ppm)	assignment[b]	(COSY) cross-peak with proton	NOE detected in difference spectra to proton	(NOESY) cross-peak with proton
0.95	**7**	6, 6′	1b, $2b_e$, 6, 6′	1b, $2b_e$, 6, 6′
2.05	**6′**	6, 7	$2b_e$, 6, 7	$2b_a$, $2b_e$, 6, 7
2.23	**6**	6′, 7	1b, 6′, 7	1b, 6′, 7
2.50	**$2b_e$**	$2a_a$, $2b_a$	*c* (under DMSO peak)	$2a_a$, $2a_e$, $2b_a$, 6′, 7
2.70	**$2b_a$**	$2a_a$, $2a_e$, $2b_e$	$2a_e$, $2b_e$, 5b, 6′	$2a_e$, $2b_e$, 5b, 6′
2.96	**$2a_a$**	$2a_e$, $2b_a$, $2b_e$	1a, $2a_e$, $2b_e$	1a, $2a_e$, $2b_e$
3.17	**$2a_e$**	$2a_a$, $2b_a$	$2a_a$, $2b_a$, $2b_e$, 5a	$2a_a$, $2b_a$, $2b_e$
4.26	**1b**	1a	1a, 6, 7	1a, 6, 7
4.37	**1a**	1b	1b, $2a_a$	1b, $2a_a$
6.24	**3a**	4a	*c*	*d*
6.27	**4a**	5a, 3a	*c*	*d*
6.37	**3b**	4b	*c*	*d*
6.44	**4b**	5b, 3b	*c*	*d*
6.94	**5a**	4a	1a, $2a_e$, 4a, 5b	4a, 5b
8.09	**5b**	4b	1b, $2b_a$, 4b, 5a	$2b_a$, 4b, 5a

[a] See Table 1. [b] See Figure 2. [c] Not irradiated. [d] Not detected.

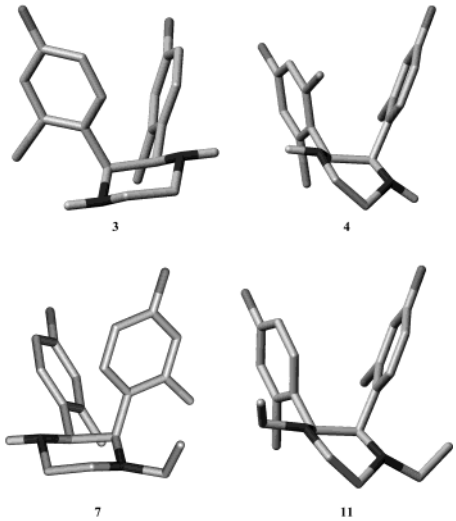

Figure 2. Low energy structure of the piperazines **3** (chair conformation) and **4** (twist conformation), the *N*-ethylpiperazine **7**, and the *N*,*N*′-diethylpiperazine **11**.

Gasteiger-Hückel charges). In contrast to the piperazines **1**−**3**, which exist in a low energetic chair conformation, for **4** as well as **5** and **6**, the twist conformation is favored. Because of van der Waals contacts between the Cl substituents and the opposite protons of the piperazine ring, the twist conformation of **5** (4.7 kJ/mol) and of **6** (10.0 kJ/mol) is of lower energy than the chair conformation. In each energetically preferred conformation, both N−H and one aryl ring are equatorially arranged (see Figure 2).

The different spatial structures of the piperazine ring influence the torsion angle between the aryl rings in **1**−**4** only marginally (47.5−47.9°) so the distances of the hydroxy groups are nearly the same (O−O distance: 6.8−7.1 Å). However, a 2,6-Cl_2 substitution in each aromatic ring as realized in **6** reduces both the torsion angle (39.4°) and the O−O-distance (6.6 Å). The latter can be distinctly surpassed by the 2,6-Cl_2-3-OH phenyl-substituted piperazine **5** during the rotation of the aromatic ring.

N-Monoalkylation also limits the dynamic of the ring inversion. The resonances of the methine protons are both split with coupling constants of $^3J = 3.8$ Hz in the spectra of **7** and **8**. This value correlates with a dihedral angle of 50−60° for the benzylic protons indicating a fixed conformation of the heterocyclic ring (Figure 1). To verify this assumption, ^{1}H NMR experiments with the (2*R*,3*S*)/(2*S*,3*R*)-*N*-ethyl-2,3-bis(2-fluoro-4-hydroxyphenyl)piperazine **7** were performed.

An appropriate experiment to determine the spatial structures of piperazines is the nuclear Overhauser enhancement experiment (NOE).[25] In the NOE as well as the NOE spectroscopy (NOESY) double-resonance experiments, a saturation transfer is achieved between protons that are closer to each other than 3.5 Å. Figure 3 shows the NOE difference spectra of **7**. The assignment of the signals is based on correlation spectroscopy (COSY) and NOE experiments (see Table 2).

H2a_e and H2b_e show NOEs to all other methylene protons while H2a_a and H2b_a possess only NOEs to H2a_e and H2b_e. Beside the NOE between H1a and H1b, strong effects are observed between H1a and H2a_a, H2b_a and H5b as well as H5a and H5b. Because of these saturation transfers, it can be concluded that the piperazine **7** takes a conformation in which the aromatic ring B is preferably arranged in axial position and the ring A is equatorially oriented (Figure 4). Only in this conformation, H5b and H2b_a as well as H1a and H2a_a came close enough to allow NOEs.

No effects are observed between H1b and H2b_e or H2a_a and H2b_a. The NOE from H5a to H2a_e is only weak in the NOE difference spectra and cannot be detected in the NOESY spectra. This is an indication but no proof that the inversion of the piperazine ring of **7** takes place only in limited degree.

In the NOESY spectra, there are strong cross-peaks between the aromatic protons H5a and H5b and also H5b and H2b_a. The NOEs from H5a to H1a and H5b to H1b are very weak although the distance of these protons amounts to 2.4 and 2.5 Å. This indicates a conformation in which the F atoms are oriented away from the piperazine moiety. However, the rotation of the aromatic rings cannot be excluded.

The NOEs of the protons H6 and H6′ support the results of Carballeira,[21] which predict an equatorial position of N substituents. In **7**, this orientation seems to be energetically favored, too. In the case of an axially standing ethyl chain, the NOEs between H7 and H2b_e should not exist while NOEs between H6/H6′ and H1a/H2a_a should occur. From the methyl group (H7), NOEs are observed to H1b and H2b_e but not to H2b_a. This

Figure 3. ^{1}H NMR spectra and NOE difference spectra of **7** in [D_6]DMSO.

seems to be the consequence of an orientation opposite the aromatic rings.

The spatial structures of the piperazines **6** and **7** were also evaluated by theoretical methods. Both compounds can exist in several low-energy chair and twist conformations. The conformations of **7** possess in the absolute minimum nearly identical energy, while in the case of **6** the twist conformation is 3.4 kJ/mol of higher

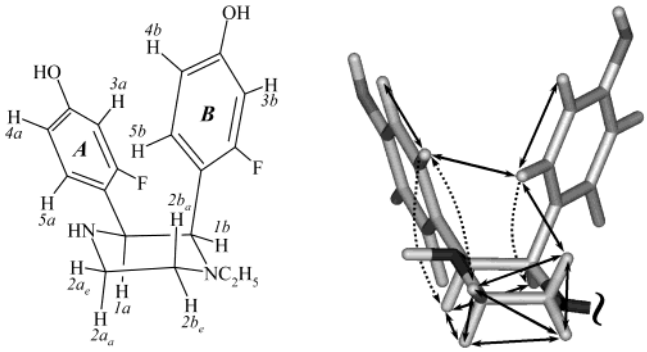

Figure 4. Postulated conformation of **7** (left) on the basis of NOE effects (right).

energy than the chair conformation. In all energetically preferred structures, the ethyl chain is equatorially arranged and the neighboring aromatic ring stands axially. The dihedral angle between the rings in piperazine **6** amounts to 45.3° with an O−O distance of 6.9 Å. For piperazine **7**, 43.7° and 6.7 Å were calculated.

Contrary to the NMR investigations in the energy minimum, the methyl group of **7** is oriented upward (Figure 2). However, the difference to a downward orientation is only 2.8 kJ/mol. In all energetically favored conformations of **6** and **7**, the protons H1a and H1b take a dihedral angle in the range of 41−48°, which correlates very well with the results determined by coupling constant analyses.

Interestingly, *N*,*N*′-diethylation increased the dynamic effects as demonstrated for the piperazines **10** and **11**. The NMR data listed in Table 1 show no splitting of the methylene and methine protons and point out dynamic effects and conversion of the piperazine ring.

The resonances of the aromatic protons H5a and H5b ($\delta = 7.45$) in the spectra of **11** are broadened (Figure 5), due to a hindered rotation at room temperature (296 K). Heating to 323 K gives a sharp signal with a defined coupling pattern. On the other hand, measurements at low temperature show that the dynamic of the molecule can be frozen.

Below 253 K, all methylene and methine protons become diastereotopic since the interconversion of the piperazine ring is restricted. By use of the Eyring equation

$$k = (k_b T/h)\, e^{-\Delta G^{\ddagger}/RT}$$

from the coalescence temperature ($T_c = 253 \pm 5$ K) and the distance between the methine protons H1a and H1b ($\Delta\nu = 184$ Hz), the free enthalpy of activation ($\Delta G_c^{\ddagger}$) can be calculated.[26] At the coalescence point, k_c amounts to 2.22 $\Delta\nu$ and the following equation is given:

$$\Delta G_c^{\ddagger} = RT_c \cdot \ln \frac{k_b T_c}{2.22\, h\, \Delta\nu} = 19.14 T_c \left(10.32 + \log \frac{T_c}{2.22\, \Delta\nu}\right) = 49 \pm 1.0 \text{ kJ/mol}$$

This value is in good agreement with previously published data for ring inversions. Harris et al.[27] calculated for the interconversion of the *N*,*N*′-dimethylpiperazines $G_{265K}^{\ddagger} = 52.8$ kJ/mol at $T_c = 265$ K.

On the basis of these results at room temperature, a fast interconversion of the piperazine ring with a stable equatorial position of the ethyl chains can be assumed. Because **10** and **11** show comparable ^{1}H NMR spectra, we postulate similar spatial structures in solution.

Theoretical considerations indicate great similarities to the *N*-monoethyl and the nonalkyl-substituted 2,3-diarylpiperazines. We calculated a spatial structure in the absolute minimum of energy with a twist conformation of the heterocyclic ring and equatorial orientations of both ethyl chains and one aromatic ring (the chair conformation would enhance the energy level of **10** by 3.7 kJ/mol and of **11** by 5.4 kJ/mol). The dihedral angle between the aryl rings in **10** and **11** amounts to 45.3−43.7° with O−O distances of 6.7 and 6.5 Å, respectively.

Biological Properties. The binding affinity to the ER (RBA) was determined for all compounds in a competition experiment using calf uterine cytosol.[28] In this test, the amount of displaced [^{3}H]**E2** from the receptor was measured. Therefore, the RBA value is an indication to which extent the compound can compete with **E2** for the binding to the ER.

To quantify the ligand-induced gene activation, the MCF-7-2a cell line was used.[29] These ER-containing mammary carcinoma cells were stably transfected with the plasmid ERE$_{wtc}$luc. The plasmid contains the "estrogen response element" of the DNA as an enhancer sequence and a reporter sequence, which codes for luciferase. The binding of ER/drug conjugate dimers leads to expression of luciferase, which correlates very well with the estrogenic potency of the drug.[30]

The nonalkylated piperazines **1**−**6** showed, with the exception of **6** (RBA = 0.05%), no significant displacement of **E2** from its binding site (RBA < 0.02%). *N*-Monoethylation of **2** and **3** increased the RBA to 0.06 (**7**) and 0.42% (**8**), while an additional ethyl group at the second piperazine nitrogen reduced the RBA values by half to 0.03 (**10**) and 0.17% (**11**). On the other hand, O methylation led in each case to a complete loss of ER interaction.

The hydroxy- and the methoxy-substituted piperazines were tested in a concentration-dependent manner (10^{-10} to 10^{-6} M) in the luciferase assay on the MCF-7-2a cell line. The maximum effects were obtained at the highest concentration used (1 μM). The results listed in Table 3 show that the halogen/hydroxy substitution pattern in the aromatic rings is essential for estrogenic activity. The Cl-substituted compounds (**3**, **8**, and **11**) were more active than the respective F-substituted ones (**2**, **7**, and **10**). Furthermore, the relative activation correlates with the number of chlorine atoms (relative activation of **3** < **4** < **6**). Interestingly, *N*-monoethylation of **3** has the same effects as the introduction of a fourth Cl substituent (**E2**, activation 100%; **8**, relative activation 74%; **6**, relative activation 73%). The *N*,*N*′-diethylated piperazine **10** was inactive (relative activation 4%), and **11** reached a relative activation of 37%, which is half of its monoethyl congener.

Discussion

We have synthesized a series of 2,3-diarylpiperazines and investigated their binding to the ER as well as their effects on the MCF-7-2a cell line. Because ligand-

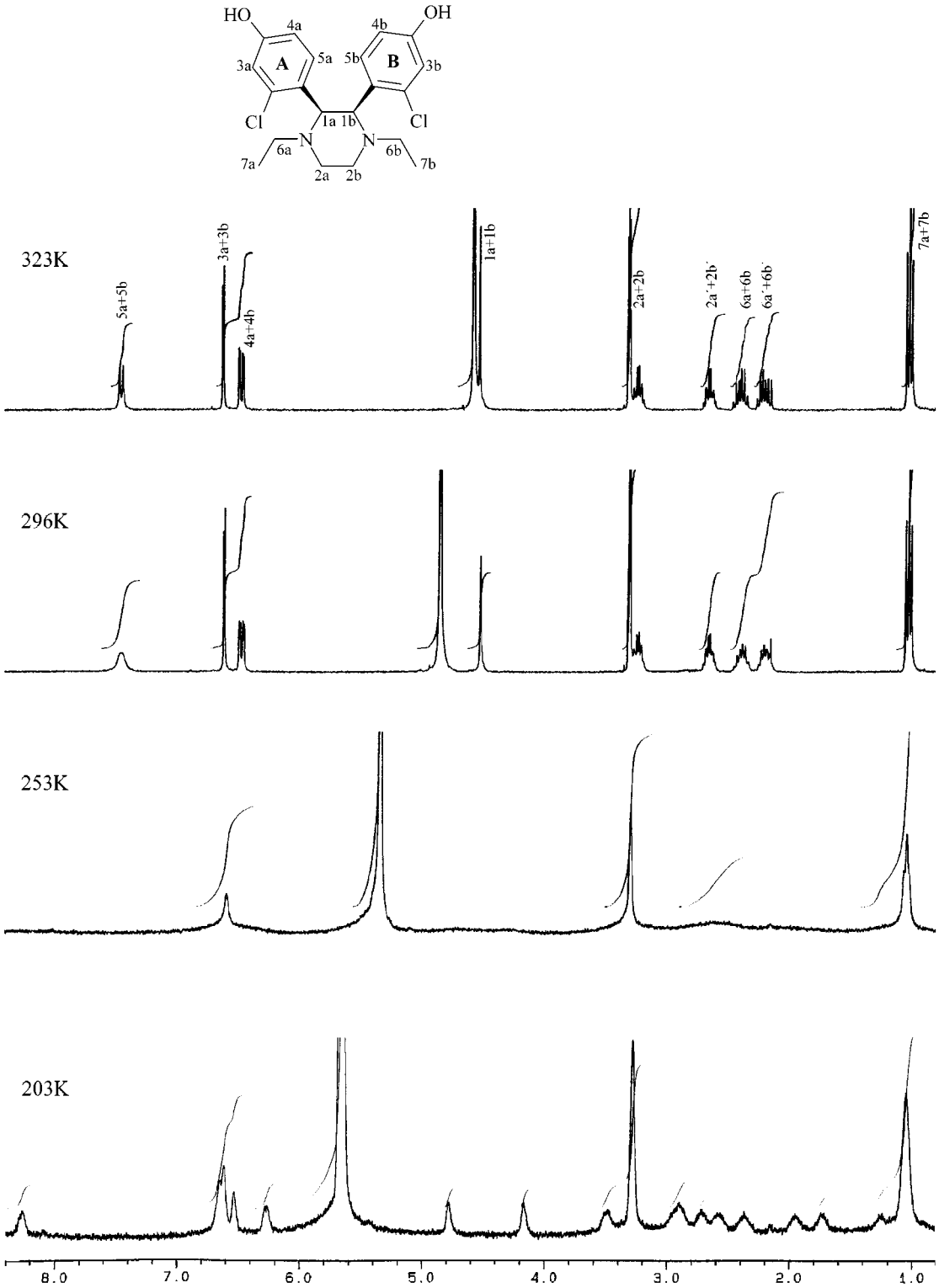

Figure 5. ^{1}H NMR spectra (300 MHz) of the piperazine **11** in [D_4]methanol at 323, 296, 253, and 203 K.

independent activation of the ER molecule can be excluded, the luciferase expression is the consequence of the interaction of the piperazines with the ligand-binding domain (LBD). In the LBD, however, an anchorage different from that of **E2** is assumed, since none of the new compounds can displace **E2** effectively from its binding site as demonstrated in the competition experiment with [^{3}H]**E2**.

The structural prerequisite for the interactions of the new compounds in the LBD can be deduced from the in vitro results. The relevance of H bridges for the ER binding documents the inactivity of all OCH_3 derivatives. Furthermore, the position of the hydroxy groups plays an important role. The shift of the OH from the 4- into the 3-position reduces the relative activation from 73 to 12%. The shielding of the hydrophilic N atoms by ortho-standing halide substituents or by *N*-alkylation elevates the luciferase expression indicating the importance of hydrophobic interactions between ligand and protein areas for the binding to the ER

Table 3. ER Affinity and Transcription Efficacy in MCF-7-2a, **1**−**11**, (**1a**−**11a**)

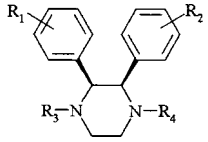

	R_1	R_2	R_3	R_4	RBA[a]	relative activation[b] (% of E_2) of luciferase expression at 10^{-6} M	
							-OCH_3 derivatives
1	4-OH	4-OH	H	H	<0.02	−1	5
2	2-F, 4-OH	2-F, 4-OH	H	H	<0.02	4	4
3	2-Cl, 4-OH	2-Cl, 4-OH	H	H	<0.02	7	1
4	2,6-Cl_2, 4-OH	2-Cl, 4-OH	H	H	<0.02	20	3
5	2,6-Cl_2, 3-OH	2,6-Cl_2, 3-OH	H	H	<0.02	12	8
6	2,6-Cl_2, 4-OH	2,6-Cl_2, 4-OH	H	H	0.05	73	5
7	2-F, 4-OH	2-F, 4-OH	ethyl	H	0.06	34	3
8	2-Cl, 4-OH	2-Cl, 4-OH	ethyl	H	0.42	74	4
9	4-OH	4-OH	ethyl	ethyl	<0.02	8	4
10	2-F, 4-OH	2-F, 4-OH	ethyl	ethyl	0.03	4	7
11	2-Cl, 4-OH	2-Cl, 4-OH	ethyl	ethyl	0.17	37	0

[a] Relative binding affinity (RBA), % = $[E_2]/[I] \times 100$; $[E_2]$ and [I] are the molar concentrations of nonradioactive E_2 and inhibitor required to decrease the bound radioactivity by 50%; $E_2 = 17\beta$-estradiol. Mean value of three determinations. [b] Values are means of three independent experiments.

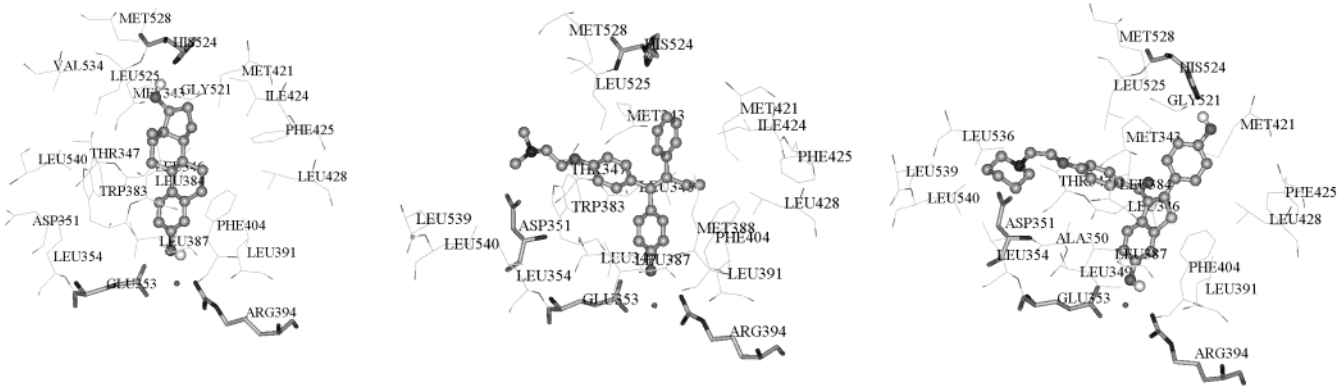

Figure 6. Interactions of estradiol (left), raloxifene (right), and 4-hydroxytamoxifen (middle) in the LBD of the ER according to Brzozowski[30] and Shiau.[32]

(relative activation: **6**, 73%; **7**, 34%; **8**, 74%). Introduction of a second ethyl chain in **7** and **8** decreases the expression of luciferase (relative activation: **10**, 4%; **11**, 37%), which leads to the suggestion that probably steric effects abolish the hydrophobic contacts to the ER.

During the past decades, many structure−activity relationship studies (SAR) on hormonally active compounds were performed to characterize the LBD. Meanwhile, the LBD/**E2** conjugate could be crystallized and analyzed by X-ray analysis[31,32] allowing an insight into the binding mode of **E2** and related compounds.

The selective hormone recognition by the ER occurs by a combination of H bonding and hydrophobic contacts. The phenolic OH group of **E2** is bound by hydrogen bridges to the γ-carboxylate of Glu 353, the guanidinium residue of Arg 394 and a water molecule. The 17β-OH group is linked to His 524. Furthermore, hydrophobic interactions with aliphatic residues of amino acids above and below the steroidal skeleton (Figure 6) are essential.

Structure−activity studies together with available X-ray data of LBD/drug conjugates revealed that drugs with high RBA values possess comparable van der Waals volumes and activate the ER by attachment to identical binding sites. These drugs (type I estrogens) must have a planar structure having two OH groups in a distance comparable to **E2** (10.9 Å).

Because of their different geometry, the estrogenically active 2,3-diarylpiperazines were assigned to a second class of estrogens (type II estrogens).[16] An interaction in the LBD comparable to that of **E2** is impossible. Therefore, a speculative binding model was derived from the crystal structure of the LBD cocrystallized with **E2**, raloxifene (RAL),[31] and 4-hydroxytamoxifen (**4OHT**)[32] (see Chart 1 and Figure 6).

RAL is attached to the LBD comparable to **E2** by hydrophilic and hydrophobic interactions.[31] Beside the H bridges known from **E2** (see Figure 6), an additional H bond is built in a narrow side pocket from the piperidine nitrogen of the side chain of RAL to Asp 351.

4OHT is also attached to Glu 353, Arg 394, a water molecule (phenolic OH), and to Asp 351 (dimethylamino group of the side chain). The missing H bridge to His 524 seems to be compensated by van der Waals contacts of the hydrophobic unsubstituted 2-phenyl ring.[33]

Further information about ligand−ER interactions is given by structure−activity studies in the class of estrogenically and antiestrogenically active 7α- and 11β-substituted **E2** derivatives.[12,34−38] Because of the steroidal skeleton, these compounds should bind in the same region of the LBD as **E2**. Large side chains at C-7 or C-11 can be positioned in analogy to a "one pocket" model.[39,40] In the case of a C-7 substitution, the steroid has to rotate around a virtual C_2 symmetry axis between C-3 and C-17 (Figure 7). Hereby, the 7α- and the 11β-

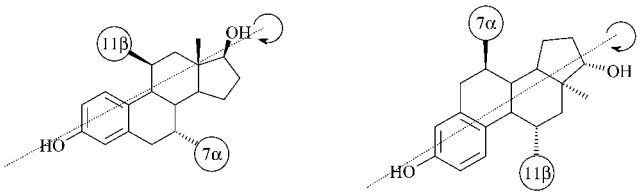

Figure 7. Orientation of 7α- and 11β-substituted **E2** derivatives at the ER.

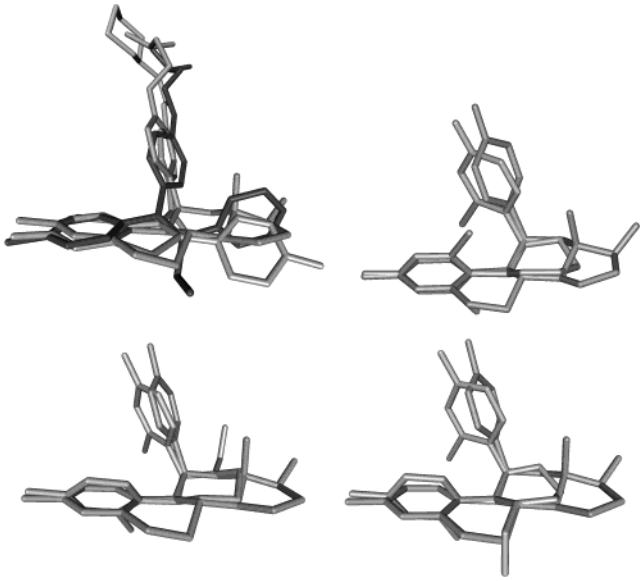

Figure 8. Superposition of low energy structures of raloxifene, 4-hydroxytamoxifen, and RU 39411 (upper left), 11β-(4-hydroxyphenyl)estradiol and piperazine **4** (twist conformation) (upper right), and the enantiomers of **8** and 11β-(4-hydroxyphenyl)estradiol.

positions become nearly equivalent for the binding at the ER.

Substitution with hydrophobic groups at either the 7α- or the 11β-position leads to compounds with essentially the same binding affinities.[39] This suggests that these compounds may interact with the same hydrophobic region in the LBD. Polar groups at the 7α- and 11β-positions decrease the RBA value depending on the distance from the **E2** core.[38]

If both the 7α- and the 11β-position in **E2** are substituted, the residue at C-7 has to be relatively small. Otherwise, the orientation of a large moiety analogous to the basic side chain of RAL in the side pocket appears to be prevented.[40] The (4-dimethylaminoethoxyphenyl) residue is well-tolerated in both the 7α- (RBA = 87%) and the 11β-position (RBA = 130%). The binding affinity of 11β-(4-dimethylaminoethoxyphenyl)−**E2** (RU 39411) surpasses even that of **E2**.

RU 39411 (see Chart 1) shows a good structural analogy to RAL, **4OHT**, and the 2,3-diarylpiperazine **4** (Figure 8). A superposition of the 11β-(4-hydroxyphenyl)−**E2** moiety with **4** indicates an orientation of the 2-chloro-4-hydroxyphenyl ring in the side pocket. Although the amino acid Asp 351 was identified as an essential anchor for antiestrogens (the binding of the basic side chains of antiestrogens leads to a displacement of the helix 12 away from the side pocket), the spatial structure of 2,3-diarylpiperazines (type II estrogens) also allows de facto the contact to Asp 351. However, a displacement of helix 12 from its normal,

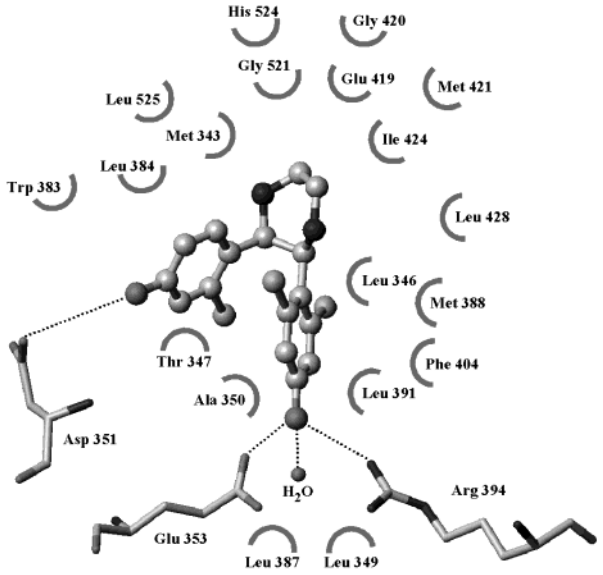

Figure 9. Postulated interactions of piperazine **4** in the LBD of the ER.

active position can be excluded, since **4** causes an activation of the luciferase gene but not an inhibition of the agonistic effects of **E2** in our test model.

N-Monoethylated piperazines exist as a mixture of enantiomers, since the ethyl residue can be located either at N-1 or at N-4 of the piperazine ring as well. According to Figure 8, the ethyl group imitates the hydrophobic 13β-methyl group of **E2** or an alkyl chain at C-7. The hydrophobic interaction is strengthened in this region of the LBD, and the binding affinity increases. Reduced activity after *N*,*N*′-diethyl substitution could be interpreted as a steric hindrance during ER binding comparable to 7α,11β-disubstituted **E2** derivatives.[38,40]

Figure 9 presents a theoretical binding mode of 2,3-diarylpiperazines in the LBD. The molecule is positioned in such a way that H bridges to Glu 353, Arg 394, and H_2O are possible. The OH group of the other aromatic ring interacts with Asp 351. Hydrophobic parts of the molecule, in particular the ortho-Cl substituents or the *N*-ethyl chain, are in van der Waals contacts with hydrophobic residues of amino acids in the LBD.

The significance of Asp 351 for estrogenic as well as antiestrogenic properties of RAL, **4OHT**, and related compounds has been verified by the group of Jordan.[41,42] They hypothesized that alterations in the charge of the amino acid 351 and changes in the interaction with the side chain of antiestrogens are critical for the estrogenicity of the ER/drug complex. This is confirmed by the effects of RAL and **4OHT** in an assay using the induction of mRNA for the TGFα gene in MDA-MB-231 breast cancer cells stably transfected with the cDNA for the wild-type Asp351 ER and the mutant Asp351Tyr ER (Tyr 351 instead of Asp 351). In this test, the Asp351Tyr ER can enhance the estrogenic properties of **4OHT** and change the pharmacology of RAL by converting it from antiestrogen to estrogen.

On the other hand, substitution of glycine for aspartate at position 351 (Asp351Gly) changed the activity of the ER/**4OHT** complex from estrogen-like to completely antiestrogenic. In the same assay, **4OHTPP**, a nonisomerizable derivative of tamoxifen without a basic

side chain (see Chart 1), shows no estrogenic properties although it is an estrogen by use of Asp351 ER. In contrast to **E2** and DES, the triphenylethylene derivatives activate gene expression and coactivator binding not through the activation function AF2 but through AF2b, a novel binding site for coactivators.[42]

On the basis of these data, Jordan et al. proposed a classification of estrogens.[43] Class I estrogens are planar and related to **E2** and DES (type I estrogens) and can easily be sealed within the hydrophobic pocket by helix 12. They will use the AF2 coactivator binding site, which will synergize AF1 to produce optimal estrogen-like action. **4OHTPP** and related angular triphenylethylenes are class II estrogens (type II estrogens) and use AF2b, which includes acidic surface amino acids on a repositioned helix 12, an exposed aspartate at position 351 and AF1.[43] This classification of estrogens correlates very well with our investigations, wherein we assume a comparable mode of action for our hormonally active piperazines, imidazoline, or imidazoles.[16]

Materials and Methods

General Procedures. IR spectra (KBr pellets): Perkin-Elmer model 580 A. ^{1}H NMR: Bruker ADX 400 spectrometer at 400 MHz (internal standard, tetramethylsilane (TMS)). Elemental analyses: Microlaboratory of Free University of Berlin. EI-MS spectra: CH-7A-Varian MAT (70 eV) or Kratos MS 25 RF (80 eV). All computational graphics were built using SYBYL 6.6, Tripos Inc., 1699 South Hanley Rd., St. Louis, MO, 63144. Geometry optimization was carried out using the Tripos force field within the SYBYL program, running on an INDY workstation. Liquid Scintillation Counter: 1450 Microbeta Plus (Wallac, Finland). Microlumat: LB 96 P (EG & G Berthold, Germany).

Syntheses. (1*R*,2*S*)/(1*S*,2*R*)-1,2-Diarylethylenediamines **1b**−**6b** were synthesized as described previously.[18−20]

General Procedure for the Synthesis of 2,3-Diarylpiperazines (Method A). To a solution of the respective 1,2-diarylethylenediamine **1b**−**6b** in dry 1,4-dioxane, dimethyl oxalate was added and heated to reflux. Subsequently, the solvent was evaporated and the crude product was dried. To the 5,6-diarylpiperazine-2,3-dione, suspended in 20 mL of dry THF, was added under nitrogen atmosphere 5 mL of a 1 M boran·THF complex. After the mixture was heated to reflux for 12 h, it was hydrolyzed with 10 mL of water and 10 mL of 3 N HCl. The THF was distilled off, and the acidic solution was heated for an additional hour. After it was cooled to room temperature, the aqueous solution was shaken with diethyl ether and alkalized with NaOH (20%), and the product was extracted with CH_2Cl_2. The organic layer was dried over Na_2SO_4 and evaporated to dryness.

(2*R*,3*S*)/(2*S*,3*R*)-2,3-Bis(4-methoxyphenyl)piperazine (1a). (1*R*,2*S*)/(1*S*,2*R*)-1,2-Bis(4-methoxyphenyl)ethylenediamine **1b**: 12.0 mmol (3.27 g). Reaction time: 12 h. Purification: chromatography on silica gel with methanol. Yield: 6.51 mmol (1.94 g), 54%, colorless oil. IR (KBr): $\bar{\nu}$ = 3436 s, br (NH); 2833 w (OCH_3); 1611 s; 1511 m; 1458 w; 1249 s; 1176 m; 1031 m; 831 m; 803 w. ^{1}H NMR ($CDCl_3$): δ 1.87 (s, 2H, N*H*,); 2.88−2.98 (m, 2H, NCH_2C); 3.24−3.35 (m, 2H, NCH_2C); 3.70 (s, 6H, OCH_3); 4.21 (s, 2H, ArC*H*); 6.69 (AA′*BB*′, ^3J = 8.8 Hz, 4H, Ar*H*-3, Ar*H*-5); 7.33 (*AA*′BB′, ^3J = 8.8 Hz, 4H, Ar*H*-2, Ar*H*-6).

(2*R*,3*S*)/(2*S*,3*R*)-2,3-Bis(2-fluoro-4-methoxyphenyl)piperazine (2a). (1*R*,2*S*)/(1*S*,2*R*)-1,2-Bis(2-fluoro-4-methoxyphenyl)ethylenediamine **2b**: 7.14 mmol (2.20 g). Reaction time: 48 h. Purification: chromatography on silica gel with diethyl ether/methanol 4 + 1. Yield: 1.98 mmol (661 mg), 28%, colorless crystals, mp 53−55 °C. IR (KBr): $\bar{\nu}$ = 3440 m, br (NH); 3415 m, br (NH); 2837 m (OCH_3); 1624 s; 1582 m; 1507 s; 1444 m; 1288 s; 1192 m; 1154 s; 1133 m; 1100 s; 1032 s; 950 m; 838 m. ^{1}H NMR ($CDCl_3$): δ 1.75 (s, 2H, N*H*); 2.91−3.03 (m, 2H, NCH_2C); 3.20−3.27 (m, 2H, NCH_2C); 3.71 (s, 6H, OCH_3); 4.66 (s, 2H, ArC*H*); 6.46 (dd, ^{3}J(H, F) = 12.4 Hz, ^4J = 2.5 Hz, 2H, Ar*H*-3); 6.51 (dd, ^3J = 8.7 Hz, ^4J = 2.5 Hz, 2H, Ar*H*-5); 7.80 (dd, ^3J = 8.7 Hz, ^{4}J(H, F) = 8.7 Hz, 2H, Ar*H*-6).

(2*R*,3*S*)/(2*S*,3*R*)-2,3-Bis(2-chloro-4-methoxyphenyl)piperazine (3a). (1*R*,2*S*)/(1*S*,2*R*)-1,2-Bis(2-chloro-4-methoxyphenyl)ethylenediamine **3b**: 5.84 mmol (2.00 g). Reaction time: 48 h. Purification: recrystalization from $CHCl_3$/diethyl ether. Yield: 3.72 mmol (1.20 g), 56%, colorless powder, mp 159−160 °C. IR (KBr): $\bar{\nu}$ = 3438 s, br (NH); 2837 w (OCH_3); 1606 s; 1493 s; 1458 m; 1285 m; 1235 m; 1125 m; 1040 s; 862 m; 826 m. ^{1}H NMR ($CDCl_3$): δ 1.70 (s, 2H, N*H*); 2.92−3.00 (m, 2H, NCH_2C); 3.19−3.26 (m, 2H, NCH_2C); 3.71 (s, 6H, OCH_3); 4.87 (s, 2H, ArC*H*); 6.64 (dd, ^3J = 8.8 Hz, ^4J = 2.7 Hz, 2H, ArC*H*-5); 6.78 (d, ^4J = 2.7 Hz, 2H, Ar*H*-3); 7.99 (d, ^3J = 8.8 Hz, 2H, Ar*H*-6).

(2*R*,3*S*)/(2*S*,3*R*)-2-(2-Chloro-4-methoxyphenyl)-3-(2,6-dichloro-4-methoxyphenyl)piperazine (4a). (1*R*,2*S*)/(1*S*,2*R*)-1-(2-Chloro-4-methoxyphenyl)-2-(2,6-dichloro-4-methoxyphenyl)-ethylenediamine **4b**: 1.06 mmol (400 mg). Reaction time: 72 h. Purification: chromatography on silica gel with diethyl ether/methanol (4 + 1). Yield: 0.199 mmol (80 mg), 19%, yellow oil. ^{1}H NMR ($CDCl_3$): δ 2.30 (s, 2H, N*H*); 2.75−3.70 (m, 4H, NCH_2C); 3.75 (s, 3H, OCH_3); 3.80 (s, 3H, OCH_3); 4.90 (d, ^3J = 5 Hz, 1H, ArC*H*); 5.10 (d, ^3J = 5 Hz, 1H, ArC*H*); 6.70−7.00 (m, 4H, Ar*H*-3, Ar*H*-5, Ar′*H*); 8.20 (d, ^3J = 8 Hz, 1H, Ar*H*-6).

(2*R*,3*S*)/(2*S*,3*R*)-2,3-Bis(2,6-dichloro-3-methoxyphenyl)-piperazine (5a). (1*R*,2*S*)/(1*S*,2*R*)-1,2-Bis(2,6-dichloro-3-methoxyphenyl)ethylenediamine **5b**: 1.46 mmol (600 mg). Reaction time: 5 days. Purification: chromatography on silicagel with CH_2Cl_2/methanol (29 + 1). Yield: 0.275 mmol (120 mg), 19%, yellow crystals, mp 79−81 °C. IR (KBr): $\bar{\nu}$ = 3435 s, br (NH); 1630 s; 1459 m; 1436 m; 1282 s; 1110 m; 1070 m; 804 m. ^{1}H NMR ($CDCl_3$): δ 2.45 (s, 2H, N*H*); 3.13−3.25 (m, 2H, NCH_2C); 3.31−3.43 (m, 2H, NCH_2C); 3.79 (s, 6H, OCH_3); 5.41 (s, 2H, ArC*H*); 6.68 (d, ^3J = 8.9 Hz, 2H, Ar*H*-4); 7.07 (d, ^3J = 8.9 Hz, 2H, Ar*H*-5).

(2*R*,3*S*)/(2*S*,3*R*)-2,3-Bis(2,6-dichloro-4-methoxyphenyl)-piperazine (6a). (1*R*,2*S*)/(1*S*,2*R*)-1,2-Bis(2,6-dichloro-4-methoxyphenyl)ethylenediamine **6b**: 1.46 mmol (600 mg). Reaction time: 5 days. Purification: chromatography on silica gel with CH_2Cl_2/methanol (29 + 1). Yield: 0.410 mmol (179 mg), 28%, yellow powder, mp 78−79 °C. IR (KBr): $\bar{\nu}$ = 3432 m, br (NH); 3411 m, br (NH); 2836 w (OCH_3); 1601 s; 1554 s; 1465 m; 1431 m; 1270 m; 1172 w; 1112 w; 1041 s; 906 w; 839 m; 793 m. ^{1}H NMR ($CDCl_3$): δ 2.54 (s, 2H, N*H*); 3.09−3.23 (m, 2H, NCH_2C); 3.28−3.43 (m, 2H, NCH_2C); 3.73 (s, 6H, OCH_3); 5.24 (s, 2H, ArC*H*); 6.69 (s, 4H, Ar*H*).

General Procedure for the Synthesis of *N*,*N*′-Diacetyl-2,3-diarylpiperazines (Method B). Under nitrogen atmosphere, acetic anhydride (5 mmol) in 15 mL of dry THF was added at −10 °C to a solution of the respective piperazine **1a**−**3a** dissolved in 5 mL of dry THF. After the mixture was heated to reflux, the reaction mixture was evaporated to dryness.

(2*R*,3*S*)/(2*S*,3*R*)-*N*,*N*′-Diacetyl-2,3-bis(4-methoxyphenyl)-piperazine (1c). (2*R*,3*S*)/(2*S*,3*R*)-2,3-Bis(4-methoxyphenyl)-piperazine **1a**: 1 mmol (298 mg). Reaction time: 1 h. Purification: chromatography on silica gel with diethyl ether/methanol 4 + 1. Yield: 0.662 mmol (253 mg), 66%, colorless powder, mp 74−76 °C. ^{1}H NMR ([D$_4$]methanol): δ 1.99 (br, 6H, CH_3CO); 3.73 (s, 6H, OCH_3); 3.88 (br, 2H, NCH_2C); 4.23 (br, 2H, NCH_2C); 5.63 (br, 2H, ArC*H*); 6.74 (AA′BB′, br, 4H, Ar*H*).

(2*R*,3*S*)/(2*S*,3*R*)-*N*,*N*′-Diacetyl-2,3-bis(2-fluoro-4-methoxyphenyl)piperazine (2c). (2*R*,3*S*)/(2*S*,3*R*)-2,3-Bis(2-fluoro-4-methoxyphenyl)piperazine **2a**: 1.18 mmol (396 mg). Reaction time: 16 h. Purification: chromatography with diethyl ether/methanol 2 + 1. Yield: 0.956 mmol (400 mg), 81%, colorless powder, mp 78−81 °C. ^{1}H NMR ($CDCl_3$): δ 1.99 (s, 6H, CH_3-CO); 3.73 (s, 6H, OCH_3); 3.78−3.93 (m, 2H, NCH_2C); 4.32 (br, 2H, NCH_2C); 5.86 (br, 2H, ArC*H*); 6.38 (dd, ^{3}J(H, F) = 12.3 Hz, ^4J = 2.3 Hz, 2H, Ar*H*-3); 6.51 (dd, ^3J = 8.7 Hz, ^4J = 2.3 Hz, 2H, Ar*H*-5); 6.86 (dd, ^3J = 8.7 Hz, ^{4}J(H, F) = 8.6 Hz, 2H, Ar*H*-6).

(2*R*,3*S*)/(2*S*,3*R*)-*N*,*N*′-Diacetyl-2,3-bis(2-chloro-4-methoxyphenyl)piperazine (3c). (2*R*,3*S*)/(2*S*,3*R*)-2,3-Bis(2-chloro-4-methoxyphenyl)piperazine **3a**: 1.63 mmol (600 mg). Reaction time: 16 h. Purification: chromatography on silica gel with diethyl ether/methanol 10 + 1. Yield: 1.55 mmol (698 mg), 95%, colorless powder, mp 165−168 °C. ^{1}H NMR ($CDCl_3$): δ 1.94 (s, 6H, CH_3CO); 3.75 (s, 6H, OCH_3); 3.85−3.97 (m, 2H, NCH_2C); 4.34 (br, 2H, NCH_2C); 5.99 (br, 2H, ArC*H*); 6.62 (dd, ^3J = 8.8 Hz, ^4J = 2.6 Hz, 2H, Ar*H*-5); 6.71 (d, ^4J = 2.6 Hz, 2H, Ar*H*-3); 6.87 (d, ^3J = 8.8 Hz, 2H, Ar*H*-6).

Reduction of the Amide Structure of the (2*R*,3*S*)/(2*S*,3*R*)-*N*,*N*′-Diacetyl-2,3-diarylpiperazines According to Method A. (2*R*,3*S*)/(2*S*,3*R*)-*N*,*N*′-Diethyl-2,3-bis(4-methoxyphenyl)piperazine (9a). (2*R*,3*S*)/(2*S*,3*R*)-*N*,*N*′-Diacetyl-2,3-bis(4-methoxyphenyl)piperazine **1c**: 0.662 mmol (253 mg). Purification: chromatography on silica gel with methanol. Yield: 0.522 mmol (185 mg), 79%, yellow crystals, mp 69−71 °C. ^{1}H NMR ($CDCl_3$): δ 1.01 (t, ^3J = 7.1 Hz, 6H, CH_3-CH_2); 2.03−2.12 (m, 2H, CH_3CH_2); 2.25−2.45 (m, 2H, CH_3CH_2); 2.55−2.60 (m, 2H, NCH_2C); 3.10−3.15 (m, 2H, NCH_2C); 3.72 (s, 6H, OCH_3); 3.75 (s, 2H, ArC*H*); 6.64 (AA′*BB*′, ^3J = 8.5 Hz, 4H, Ar*H*-3, Ar*H*-5); 7.15 (*AA*′BB′, br, 4H, Ar*H*-2, Ar*H*-6).

(2*R*,3*S*)/(2*S*,3*R*)-*N*-Ethyl-2,3-bis(2-fluoro-4-methoxyphenyl)piperazine (7a) and (2*R*,3*S*)/(2*S*,3*R*)-*N*,*N*′-Diethyl-2,3-bis(2-fluoro-4-methoxyphenyl)piperazine (10a). (2*R*,3*S*)/(2*S*,3*R*)-*N*,*N*′-Diacetyl-2,3-bis(2-fluoro-4-methoxyphenyl)piperazine **2c**: 0.956 mmol (400 mg). Separation: chromatography on silica gel with diethyl ether.

(2*R*,3*S*)/(2*S*,3*R*)-*N*-Ethyl-2,3-bis(2-fluoro-4-methoxyphenyl)piperazin (7a). Yield: 0.259 mmol (94 mg), 27%, colorless oil. ^{1}H NMR ($CDCl_3$): δ 1.05 (t, ^3J = 7.2 Hz, 3H, CH_3-CH_2); 2.16−2.25 (m, 1H, CH_3CH_2); 2.36−2.45 (m, 1H, CH_3CH_2); 2.63−2.69 (m, 1H, NCH_2C); 2.88−2.95 (m, 1H, NCH_2C); 3.19−3.26 (m, 1H, NCH_2C); 3.31−3.37 (m, 1H, NCH_2C); 3.69 (s, 3H, OCH_3); 3.71 (s, 3H, OCH_3); 4.51 (d, ^3J = 3.7 Hz, 1H, ArC*H*); 4.68 (d, ^3J = 3.7 Hz, 1H, ArC*H*); 6.33−6.39 (m, 2H, Ar*H*-3, Ar*H*-5); 6.47 (dd, ^{3}J(H, F) = 12.3 Hz, ^4J = 2.5 Hz, 1H, Ar*H*-3); 6.56 (dd, ^3J = 8.7 Hz, ^4J = 2.5 Hz, 1H, Ar*H*-5); 7.08 (dd, ^3J = 8.6 Hz, ^{4}J(H, F) = 8.6 Hz, 1H, Ar*H*-6); 8.16 (dd, ^3J = 8.5 Hz, ^{4}J(H, F) = 8.5 Hz, 1H, Ar*H*-6).

(2*R*,3*S*)/(2*S*,3*R*)-*N*,*N*′-Diethyl-2,3-bis(2-fluoro-4-methoxyphenyl)piperazine (10a). Yield: 0.538 mmol (210 mg), 56%, colorless oil. ^{1}H NMR ($CDCl_3$): δ 1.05 (t, ^3J = 7.2 Hz, 6H, CH_3-CH_2); 2.13−2.22 (m, 2H, CH_3CH_2); 2.33−2.43 (m, 2H, CH_3CH_2); 2.60−2.65 (m, 2H, NCH_2C); 3.09−3.15 (m, 2H, NCH_2C); 3.73 (s, 6H, OCH_3); 4.32 (s, 2H, ArC*H*); 6.43 (dd, ^{3}J(H, F) = 12.2 Hz, ^4J = 2.4 Hz, 2H, Ar*H*-3); 6.48 (dd, ^3J = 8.7 Hz, ^4J = 2.4 Hz, 2H, Ar*H*-5); 7.56 (br, 2H, Ar*H*-6).

(2*R*,3*S*)/(2*S*,3*R*)-*N*-Ethyl-2,3-bis(2-chloro-4-methoxyphenyl)piperazine (8a) and (2*R*,3*S*)/(2*S*,3*R*)-*N*,*N*′-Diethyl-2,3-bis(2-chloro-4-methoxyphenyl)piperazine (11a). (2*R*,3*S*)/(2*S*,3*R*)-*N*,*N*′-Diacetyl-2,3-bis(2-chloro-4-methoxyphenyl)piperazine **3c**: 1.55 mmol (698 mg). Separation: chromatography on silica gel with diethyl ether.

(2*R*,3*S*)/(2*S*,3*R*)-*N*-Ethyl-2,3-bis(2-chloro-4-methoxyphenyl)piperazine (8a). Yield: 0.354 mmol (140 mg), 23%, colorless oil. ^{1}H NMR ($CDCl_3$): δ 1.05 (t, ^3J = 7.2 Hz, 3H, CH_3-CH_2); 2.23−2.32 (m, 1H, CH_3CH_2); 2.41−2.50 (m, 1H, CH_3CH_2); 2.69−2.73 (m, 1H, NCH_2C); 3.05−3.13 (m, 1H, NCH_2C); 3.19−3.26 (m, 1H, NCH_2C); 3.32−3.39 (m, 1H, NCH_2C); 3.70 (s, 3H, OCH_3); 3.72 (s, 3H, OCH_3); 4.78 (d, ^3J = 3.6 Hz, 1H, ArC*H*); 4.83 (d, ^3J = 3.6 Hz, 1H, ArC*H*); 6.47 (dd, ^3J = 8.7 Hz, ^4J = 2.6 Hz, 1H, Ar*H*-5); 6.66 (d, ^4J = 2.6 Hz, 1H, Ar*H*-3); 6.69 (dd, ^3J = 8.7 Hz, ^4J = 2.6 Hz, 1H, Ar*H*-5); 6.78 (d, ^4J = 2.6 Hz, 1H, Ar*H*-3); 7.13 (d, ^3J = 8.7 Hz, 1H, Ar*H*-6); 8.18 (d, ^3J = 8.7 Hz, 1H, Ar*H*-6).

(2*R*,3*S*)/(2*S*,3*R*)-*N*,*N*′-Diethyl-2,3-bis(2-chloro-4-methoxyphenyl)piperazine (11a). Yield: 1.11 mmol (470 mg), 72%, colorless powder, mp 62−65 °C. ^{1}H NMR ($CDCl_3$): δ 1.02 (t, ^3J = 7.1 Hz, 6H, CH_3CH$_2$); 2.18−2.27 (m, 2H, CH_3CH_2); 2.30−2.41 (m, 2H, CH_3CH_2); 2.49−2.70 (m, 2H, NCH_2C); 3.14−3.22 (m, 2H, NCH_2C); 3.71 (s, 6H, OCH_3); 4.55 (s, 2H, ArC*H*); 6.55 (dd, ^3J = 8.8 Hz, ^4J = 2.6 Hz, 2H, Ar*H*-5); 6.70 (d, ^4J = 2.6 Hz, 2H, Ar*H*-3); 7.26 (br, 2H, Ar*H*-6).

General Procedure for the Ether Cleavage with BBr_3 (Method C). A solution of the methyl ether (1.00 mmol) in 20 mL of dry CH_2Cl_2 was cooled to −60 °C. At this temperature, BBr_3 (4.5 mmol) in 5 mL of dry CH_2Cl_2 was added under N_2 atmosphere. The reaction mixture was allowed to warm and was stirred for further 48 h. After the reaction mixture was cooled with an ice bath, surplus of BBr_3 was hydrolyzed three times with methanol and the phenolic product was dissolved in 0.1 N NaOH. The alkaline water phase was filtered, and the pH was adjusted to 8 with 2 N HCl. The precipitate was collected by suction filtration and dried over P_2O_5. Subsequently, the crude product was purified by column chromatography or fractional crystallization.

(2*R*,3*S*)/(2*S*,3*R*)-2,3-Bis(4-hydroxyphenyl)piperazine (1). (2*R*,3*S*)/(2*S*,3*R*)-2,3-Bis(4-methoxyphenyl)piperazine **1a**: 0.757 mmol (226 mg). Reaction time: 24 h at room temperature. Purification: recrystallization from methanol. Yield: 0.610 mmol (165 mg), 81%, colorless powder, mp 189−190 °C. IR (KBr): $\bar{\nu}$ = 3600−3000 m, br (OH); 1611 m; 1511 s; 1377 m; 1317 m; 1253 s; 1177 m; 891 m; 826 s. ^{1}H NMR (see Table 1). Anal. ($C_{16}H_{18}N_2O_2$) C H N.

(2*R*,3*S*)/(2*S*,3*R*)-2,3-Bis(2-fluoro-4-hydroxyphenyl)piperazine (2). (2*R*,3*S*)/(2*S*,3*R*)-2,3-Bis(2-fluoro-4-methoxyphenyl)-piperazine **2a**: 0.598 mmol (200 mg). Reaction time: 24 h at room temperature. Purification: recrystallization from methanol. Yield: 0.434 mmol (133 mg), 73%, colorless powder, mp at 210 °C under decomposition. IR (KBr): $\bar{\nu}$ = 3600−2600 m, br (OH); 1624 s; 1509 m; 1472 s; 1357 w; 1300 s; 1252 m; 1154 m; 1134 w; 1092 s; 966 s; 846 s; 817 m. MS (EI, 150 °C): *m*/*z* (%) = 306 (30) $[M]^{+\bullet}$; 276 (12); 167 (23); 153 (27); 138 (42); 112 (24); 30 (100). ^{1}H NMR (see Table 1). Anal. ($C_{16}H_{16}F_2N_2O_2$) C H N.

(2*R*,3*S*)/(2*S*,3*R*)-2,3-Bis(2-chloro-4-hydroxyphenyl)piperazine (3). (2*R*,3*S*)/(2*S*,3*R*)-2,3-Bis(2-chloro-4-methoxyphenyl)piperazine **3a**: 0.871 mmol (320 mg). Reaction time: 36 h at room temperature. Purification: recrystallization from methanol. Yield: 0.598 mmol (203 mg), 69%, colorless powder, mp at 175 °C under decomposition. IR (KBr): $\bar{\nu}$ = 3600−2700 m, br (OH); 2955 w; 1606 s; 1496 s; 1453 s; 1363 m; 1268 s; 1239 s; 1125 m; 1038 m; 900 m; 853 m. MS (EI, 180 °C): *m*/*z* (%) = 338 (24) $[M]^{+\bullet}$; 303 (2) $[M\text{-}Cl]^+$; 210 (12); 183 (42); 170 (54); 154 (100); 141 (54); 128 (22). ^{1}H NMR (see Table 1). Anal. ($C_{16}H_{16}Cl_2N_2O_2$) C H N.

(2*R*,3*S*)/(2*S*,3*R*)-2-(2-Chloro-4-hydroxyphenyl)-3-(2,6-dichloro-4-hydroxyphenyl)piperazine (4). (2*R*,3*S*)/(2*S*,3*R*)-2-(2-Chloro-4-methoxyphenyl)-3-(2,6-dichloro-4-methoxyphenyl)-piperazine **4a**: 0.212 mmol (85 mg). Reaction time: 48 h under reflux. Purification: chromatography on silica gel with diethyl ether/methanol 4 + 1. Yield: 0.099 mmol (37 mg), 47%, colorless powder, mp 148−150 °C. IR (KBr): ν 3600−2900 s, br (OH); 2943 w; 1604 s; 1493 w; 1439 s; 1379 w; 1272 s; 1234 m; 1101 m; 1039 m; 953 m; 901m; 854 m. ^{1}H NMR (see Table 1). Anal. ($C_{16}H_{15}Cl_3N_2O_2$) C H N.

(2*R*,3*S*)/(2*S*,3*R*)-2,3-Bis(2,6-dichloro-3-hydroxyphenyl)-piperazine (5). (2*R*,3*S*)/(2*S*,3*R*)-2,3-Bis(2,6-dichloro-3-methoxyphenyl)piperazine **5a**: 0.229 mmol (100 mg). Reaction time: 96 h under reflux. Purification: chromatography on silica gel with diethyl ether/methanol 10 + 1. Yield: 0.098 mmol (40 mg), 43%, yellow powder, mp 147−149 °C. IR (KBr): $\bar{\nu}$ = 3600−2900 s, br (OH); 2938 w; 1631 m; 1569 m; 1448 s; 1293 s; 1202 w; 1103 w; 815 m. ^{1}H NMR (see Table 1). Anal. ($C_{16}H_{14}Cl_4N_2O_2$) C H N.

(2*R*,3*S*)/(2*S*,3*R*)-2,3-Bis(2,6-dichloro-4-hydroxyphenyl)-piperazine (6). (2*R*,3*S*)/(2*S*,3*R*)-2,3-Bis(2,6-dichloro-4-methoxyphenyl)piperazine **6a**: 0.195 mmol (85 mg). Reaction time: 5 days under reflux. Purification: chromatography on silica gel with diethyl ether/methanol 10 + 1. Yield: 0.066 mmol (27 mg), 34%, yellow powder, mp 168−170 °C. IR (KBr): $\bar{\nu}$ = 3600−2700 s, br (OH); 2957 w; 1603 s; 1571 s; 1437 s; 1272 s; 1173 m; 1093 m; 1059 m; 952 m; 855 s; 793 s. ^{1}H NMR (see Table 1). Anal. ($C_{16}H_{14}Cl_4N_2O_2$) C H N.

(2*R*,3*S*)/(2*S*,3*R*)-*N*-Ethyl-2,3-bis(2-fluoro-4-hydroxyphenyl)piperazine (7). (2*R*,3*S*)/(2*S*,3*R*)-*N*-Ethyl-2,3-bis(2-fluoro-4-methoxyphenyl)piperazine **7a**: 0.828 mmol (300 mg).

Reaction time: 36 h at room temperature. Purification: chromatography on silica gel with acetone. Yield: 0.508 mmol (170 mg), 61%, colorless powder, mp 152−153 °C. IR (KBr): $\bar{\nu}$ = 3600−2800 s, br (OH); 1625 s; 1508 s; 1458 s; 1385 m; 1299 s; 1239 m; 1150 s; 1093 s; 967 s; 846 s. MS (EI, 150 °C): *m*/*z* (%) = 334 (6) $[M]^{+\bullet}$; 305 (10) $[M-C_2H_5]^+$; 182 (100); 168 (20); 152 (21); 138 (21); 125 (42); 58 (88). ^{1}H NMR (see Table 1). Anal. ($C_{18}H_{20}F_2N_2O_2$) C H N.

(2*R*,3*S*)/(2*S*,3*R*)-*N*-Ethyl-2,3-bis(2-chloro-4-hydroxyphenyl)piperazine (8). (2*R*,3*S*)/(2*S*,3*R*)-*N*-Ethyl-2,3-bis(2-chloro-4-methoxyphenyl)piperazine **8a**: 0.354 mmol (140 mg). Reaction time: 36 h at room temperature. Purification: recrystallization from methanol. Yield: 0.150 mmol (55 mg), 42%, colorless powder, mp 178−180 °C. IR (KBr): $\bar{\nu}$ = 3600−2600 s, br (OH); 3316 m (NH); 2938 w, 2851 w; 1606 s; 1494 s; 1474 s; 1457 s; 1382 w; 1355 w; 1273 s; 1248 s; 1139 m; 1036 m; 901 s; 856 m. MS (EI, 190 °C): *m*/*z* (%) = 366 (5) $[M]^{+\bullet}$; 337 (8) $[M-C_2H_5]^+$; 210 (11); 198 (100); 184 (25); 168 (17); 155 (23); 141 (42). ^{1}H NMR (see Table 1). Anal. ($C_{18}H_{20}Cl_2N_2O_2$) C H N.

(2*R*,3*S*)/(2*S*,3*R*)-*N*,*N*′-Diethyl-2,3-bis(4-hydroxyphenyl)piperazine (9). (2*R*,3*S*)/(2*S*,3*R*)-*N*,*N*′-Diethyl-2,3-bis(4-methoxyphenyl)piperazine **9a**: 1.75 mmol (620 mg). Reaction time: 24 h at room temperature. Purification: chromatography on silica gel with methanol. Yield: 1.23 mmol (400 mg), 70%, colorless powder, mp 162−164 °C. IR (KBr): $\bar{\nu}$ = 3600−2600 s, br (OH); 2973 m; 2814 m; 1610 s; 1512 s; 1453 m; 1374 w; 1249 s; 1174 m; 1147 m; 1103 m; 836 s. MS (EI, 150 °C): *m*/*z* (%) = 326 (47) $[M]^{+\bullet}$; 297 (36) $[M-C_2H_5]^+$; 176 (100); 162 (28); 148 (41); 134 (32); 120 (14); 107 (29). ^{1}H NMR (see Table 1). Anal. ($C_{20}H_{26}N_2O_2$) C H N.

(2*R*,3*S*)/(2*S*,3*R*)-*N*,*N*′-Diethyl-2,3-bis(2-fluoro-4-hydroxyphenyl)piperazine (10). (2*R*,3*S*)/(2*S*,3*R*)-*N*,*N*′-Diethyl-2,3-bis-(2-fluoro-4-methoxyphenyl)piperazine **10a**: 0.435 mmol (170 mg). Reaction time: 36 h at room temperature. Purification: recrystallization from CH_2Cl_2/ligroin. Yield: 0.268 mmol (97 mg), 62%, colorless powder, mp 118−121 °C. IR (KBr): $\bar{\nu}$ = 3600−2600 s, br(OH); 2974 m; 2819 w; 1624 s; 1507 s; 1463 s; 1390m; 1298 s; 1242 m; 1150 s; 1090 s; 966 s; 845 s. MS (EI, 180 °C): *m*/*z* (%) = 362 (44) $[M]^{+\bullet}$; 333 (65) $[M-C_2H_5]^+$; 248 (22); 194 (100); 180 (44); 166 (72); 152 (76); 138 (25); 125 (48); 115 (82). ^{1}H NMR (see Table 1). Anal. ($C_{20}H_{24}F_2N_2O_2$) C H N.

(2*R*,3*S*)/(2*S*,3*R*)-*N*,*N*′-Diethyl-2,3-bis(2-chloro-4-hydroxyphenyl)piperazine (11). (2*R*,3*S*)/(2*S*,3*R*)-*N*,*N*′-Diethyl-2,3-bis-(2-chloro-4-methoxyphenyl)piperazine **11a**: 0.723 mmol (306 mg). Reaction time: 36 h at room temperature. Purification: chromatography on silica gel with acetone. Yield: 0.493 mmol (195 mg), 68%, colorless powder, mp 171−173 °C. IR (KBr): $\bar{\nu}$ = 3600−2700 s, br (OH); 2973 m; 2828 w; 1725 m; 1606 s; 1494 s; 1450 s; 1378 m; 1354 m; 1282 s; 1229 s; 1144 m; 1038 m; 979 w; 900 s; 853 m; 830 m. MS (EI, 180 °C): *m*/*z* (%) = 394 (25) $[M]^{+\bullet}$; 366 (35) $[M-C_2H_5]^+$; 211 (100); 197 (34); 185 (29); 177 (77); 168 (51); 154 (20); 141 (45); 115 (76). ^{1}H NMR (see Table 1). Anal. ($C_{20}H_{24}Cl_2N_2O_2$) C H N.

Biological Methods. Biochemicals, Chemicals, and Materials. Dextran, 17β-estradiol, L-glutamine (L-glutamine solution: 29.2 mg/mL phosphate-buffered saline (PBS)) and Minimum Essential Medium Eagle (EMEM) were purchased from Sigma (Munich, Germany); Dulbecco's Modified Eagle Medium without phenol red (DMEM) was from Gibco (Eggenstein, Germany); bovine calf serum (BCS) was from Bio whittaker (Verviers, Belgium); *N*-hexamethylpararosaniline (crystal violet) and gentamicin sulfate were from Fluka (Deisenhofen, Germany); glutardialdehyde (25%) was from Merck (Darmstadt, Germany); trypsin (0.05%) in ethylenediaminetetraacetic acid (0.02%) (trypsin/EDTA) was from Boehringer (Mannheim, Germany); penicillin−streptomycin gold standard (10 000 IE penicillin/mL, 10 mg streptomycin/mL) and geneticin disulfate (geneticin solution: 35.71 mg/mL PBS) were from ICN Biomedicals GmbH (Eschwege, Germany); Norit A (charcoal) was from Serva (Heidelberg, Germany); cell culture lysis reagent (5×) (diluted 1:5 with purified water before use) and the luciferase assay reagent were from Promega (Heidelberg, Germany); optiphase HiSafe3 liquid scintillator was from Wallac (Turku, Finland); NET-317-estradiol[2,4,6,7-^{3}H(N)] (17β-[^{3}H]estradiol) was from Du Pont NEN (Boston, MA); $CDCl_3$, [D_6]acetone, [D_6]DMSO, and [D_4]methanol were from Aldrich (Steinheim, Germany); PBS was prepared by dissolving 8.0 g of NaCl, 0.2 g of KCl, 1.44 g of $Na_2HPO_4 \times 2\ H_2O$, and 0.2 g of KH_2PO_4 (all purchased from Merck or Fluka) in 1000 mL of purified water. TRIS- buffer (pH = 7.5) was prepared by dissolving 1.211 g of trishydroxymethylaminomethane, 0.372 24 g of Titriplex III, and 0.190 53 g of sodium azide (all from Merck or Fluka) in 1 L of purified water. Deionized water was produced by means of a Millipore Milli-Q Water System, resistivity >18 MΩ. T-75 flasks, reaction tubes, 96 well plates, and 6 well plates were purchased from Renner GmbH (Dannstadt, Germany).

ER Binding Assay. The applied method was described already by Hartmann et al.[28] and used with some modifications. The RBA of the test compounds to the ER was determined by the displacement of 17β-[^{3}H]estradiol from its binding site. For this purpose, the test compounds were dissolved in ethanol and diluted with TRIS-buffer to 6−8 appropriate concentrations (300 μL). They were incubated shaking with calf uterine cytosol (100 μL) and 17β-[^{3}H]estradiol (0.723 pmol in TRIS-buffer (100 μL); activity: 2249.4 Bq/tube) at 4 °C overnight. To stop the reaction, 500 μL of a dextran−charcoal suspension in TRIS-buffer was added to each tube. After it was shaken for 90 min at 4 °C and centrifuged, 500 μL of HiSafe3 was mixed with 100 μL of supernatant of each sample and the reactivity was determined by liquid scintillation spectroscopy. The same procedure was used to quantify the binding of 17β-[^{3}H]estradiol (0.723 pmol control). Nonspecific binding was calculated using 2 nmol of 17β-estradiol as the competing ligand. On a semilog plot, the percentage of maximum-bound labeled steroid corrected by the nonspecifically bound 17β-[^{3}H]estradiol vs concentration of the competitor (log-axis) is plotted. At least six concentrations of each compound were chosen to estimate its binding affinity. From this plot, those molar concentrations of unlabeled estradiol and of the competitors were determined, which reduced the binding of the radioligand by 50%.

$$\mathrm{RBA} = \frac{c_{[^3\mathrm{H}]\text{-estradiol}} \text{ at 50\% inhibition}}{c_{\mathrm{sample}} \text{ at 50\% inhibition}} \times 100\%$$

Luciferase Assay. The pertinent in vitro assay was described earlier by Hafner et al.[29] One week before starting the experiment, MCF-7-2a cells were cultivated in DMEM supplemented with L-glutamine, antibiotics, and dextran/charcoal-treated BCS (ct-BCS, 50 mL/L). Cells from an almost confluent monolayer were removed by trypsinization and suspended to approximately 2.2×10^5 cells/mL in the growth medium mentioned above. The cell suspension was then cultivated in six well flat-bottomed plates (0.5 mL cell suspension and 2.0 mL medium per well) at growing conditions (see above). After 24 h, 25 μL of a stock solution of the test compounds was added to achieve concentrations ranging from 10^{-5}−10^{-10} M and the plates were incubated for 50 h. Before they were harvested, the cells were washed twice with PBS and then 200 μL of cell culture lysis reagent was added into each well. After a 20 min lysation at room temperature, cells were transferred into reaction tubes and centrifugated. Luciferase was assayed using the Promega luciferase assay reagent. Fifty microliters of each supernatant was mixed with 50 μL of substrate reagent. Luminescence (in relative light units, RLU) was measured for 10 s using a microlumat. Measurements were corrected by correlating the quantity of protein (quantified according to Bradford[44]) of each sample with the mass of luciferase. Estrogenic activity was expressed as percent activation of a 10^{-8} M estradiol control (100%).

Acknowledgment. We are grateful to Prof. E. von Angerer for providing the MCF-7-2a cell line. The technical assistance of S. Bergemann and I. Schnautz is acknowledged. The presented work was supported

by Grant Gu285/3-1 from the Deutsche Forschungsgemeinschaft.

References

(1) White, R.; Parker, M. G. Molecular mechanisms of steroid hormone action. *Endocr.-Relat. Cancer* **1998**, *5*, 1−14.

(2) Tsai, M.-J.; O'Malley, B. W. Molecular mechanisms of action of steroid/thyroid receptor superfamily members. *Annu. Rev. Biochem.* **1994**, *63*, 451−486.

(3) Neven, P.; Vergote, I. Tamoxifen, screening and new oestrogen receptor modulators. *Baillieres Best Pract. Res. Clin. Obstet. Gynaecol.* **2001**, *15*, 365−380.

(4) Levenson, A. S.; Jordan, V. C. Selective oestrogen receptor modulation: molecular pharmacology for the millennium. *Eur. J. Cancer* **1999**, *35*, 1974−1985.

(5) Mitlak, B. H.; Cohen, F. J. In search of optimal long-term female hormone replacement: the potential of selective estrogen receptor modulators. *Horm. Res.* **1997**, *48*, 155−163.

(6) Cosman, F.; Lindsay, R. Selective estrogen receptor modulators: clinical spectrum. *Endocr. Rev.* **1999**, *20*, 418−434.

(7) Rizzoli, R.; Bonjour, J. P.; Ferrari, S. L. Osteoporosis, genetics and hormones. *J. Mol. Endocrinol.* **2001**, *26*, 79−94.

(8) Mendelsohn, M. E. Mechanisms of estrogen action in the cardiovascular system. *J. Steroid Biochem. Mol. Biol.* **2000**, *74*, 337−343.

(9) Brinton, R. D. Cellular and molecular mechanisms of estrogen regulation of memory function and neuroprotection against Alzheimer's disease: recent insights and remaining challenges. *Learn Mem.* **2001**, *8*, 121−133.

(10) MacGregor Schafer, J. I.; Jordan, V. C. Basic guide to the mechanisms of antiestrogen action. *Pharmacol. Rev.* **1998**, *50*, 151−196.

(11) Wakeling, A. E.; Dukes, M.; Bowler, J. A potent specific pure antiestrogen with clinical potential. *Cancer Res.* **1991**, *51*, 3867−3873.

(12) Van de Velde, P.; Nique, F.; Bouchoux, F.; Bremaud, J.; Hameau, M. C.; Lucas, D.; Moratille, C.; Viet, S.; Philibert, D.; Teutsch, G. RU 58,668, a new pure antiestrogen inducing a regression of human mammary carcinoma implanted in nude mice. *J. Steroid Biochem. Mol. Biol.* **1994**, *48*, 187−196.

(13) Levin, M.; D'Souza, N.; Castaner, J. Fulvestrant. *Drugs Future* **2001**, *26*, 841−850.

(14) Stauffer, S. R.; Coletta, C. J.; Tedesco, R.; Nishiguchi, G.; Carlson, K.; Sun, J.; Katzenellenbogen, B. S.; Katzenellenbogen, J. A. Pyrazole ligands: structure-affinity/activity relationships and estrogen receptor-α-selective agonists. *J. Med. Chem.* **2000**, *43*, 4934−4947.

(15) Henke, B. R.; Drewry, D. H.; Jones, S. A.; Stewart, E. L.; Weaver, S. L.; Wiethe, R. W. 2-Amino-4,6-diarylpyridines as novel ligands for the estrogen receptor. *Bioorg. Med. Chem. Lett.* **2001**, *11*, 1939−1942.

(16) Gust, R.; Keilitz, R.; Schmidt, K. Investigations of new lead structures for the design of selective estrogen receptor modulators. *J. Med. Chem.* **2001**, *44*, 1963−1970.

(17) Schertl, S.; Hartmann, R. W.; Batzl-Hartmann, C.; Schlemmer, R.; Spruss, T.; Bernhardt, G.; Gust, R.; Schönenberger, H. 1-(2,6-dichloro-4-hydroxyphenyl)-2-phenylethanes—new biological response modifiers for the therapy of breast cancer. Synthesis and evaluation of estrogenic/antiestrogenic properties. *Arch. Pharm.* **2001**, *334*, 125−137.

(18) Gust, R.; Burgemeister, Th.; Mannschreck, A.; Schönenberger, H. Aqua[1-(2,6-dichloro-4-hydroxyphenyl)-2-phenylethylenediamine]sulfatoplatinum(II) complexes with variable substituents in the 2-phenyl ring. 1. Synthesis and antitumor and estrogenic properties. *J. Med. Chem.* **1990**, *33*, 2535−2544.

(19) Karl, J.; Gust, R.; Spruss, T.; Schneider, M. R.; Schönenberger, H.; Engel, J.; Wrobel, K. H.; Lux, F.; Haeberlin, S. T. Ring-substituted [1,2-bis(4-hydroxyphenyl)ethylenediamine]dichloroplatinum(II) complexes: compounds with a selective effect on the hormone-dependent mammary carcinoma. *J. Med. Chem.* **1988**, *31*, 72−83.

(20) Gust, R.; Schönenberger, H. Synthesis and evaluation of the antimammary tumor activity and the estrogenic side effects of [1,2-bis(2,6-dihalo-3-hydroxyphenyl)ethylenediamine]platinum(II) complexes. *Eur. J. Med. Chem.* **1993**, *28*, 103−115.

(21) Carballeira, L.; Mosquera, R. A.; Rios, M. A.; Tovar, C. A. Conformational analysis of polyfunctional amino compounds by molecular mechanics. Part II: 1,2-ethanediamine, 1,3-propanediamine and 1,4-diazacyclohexanes. *J. Mol. Struct.* **1989**, *193*, 263−277.

(22) Gust, R.; Niebler, K.; Schönenberger, H. Investigation of the conformational influence on the hormonal activity of 1,2-bis(2,6-dichloro-4-hydroxyphenyl)ethylenediamines and of their platinum(II) complexes. Part I: synthesis, estradiol receptor affinity and estrogenic activity of diastereomeric [N-alkyl and N,N′-dialkyl-1,2-bis(2,6-dichloro-4-hydroxyphenyl)ethylenediamine]-dichloroplatinum(II) complexes. *J. Med. Chem.* **1995**, *38*, 2070−2079.

(23) Karplus, M. Vicinal proton coupling in nuclear magnetic resonance. *J. Am. Chem. Soc.* **1963**, *85*, 2870−2871.

(24) Gust, R.; Schönenberger, H.; Range, K. J.; Klement, U. Aqua[1-(2,6-dichloro-4-hydroxyphenyl)-2-phenylethylenediamine]sulfatoplatinum(II) Complexes with variable substituents in the 2-phenyl ring. Part II: Correlation of molecular structure and estrogenic activity of breast and prostate cancer inhibiting [erythro-1-(2,6-dichloro-4-hydroxyphenyl)-2-(2-halo-4-hydroxyphenyl)ethylenediamine]platinum(II) complexes. *Arch. Pharm. (Weinheim)* **1993**, *326*, 967−976.

(25) Neuhaus, D.; Williamson, T. *The Nuclear Overhauser Effect in Structure and Conformeric Analysis*; VCH: New York, 1989.

(26) Oki, M. In *Applications of Dynamic NMR Spectroscopy to Organic Chemistry*; Marchand, A. P., Ed.; VCH: Weinheim, Germany, 1985.

(27) Harris, R. K.; Spragg, R. A. Ring inversion in morpholine and piperazine derivatives studied by nuclear magnetic resonance. *Chem. Commun.* **1966**, *10*, 314−316.

(28) Hartmann, R.; Kranzfelder, G.; von Angerer, E.; Schönenberger, H. Antiestrogens. Synthesis and evaluation of mammary tumor inhibiting activity of 1,1,2,2-tetraalkyl-1,2-diphenylethanes. *J. Med. Chem.* **1980**, *23*, 841−848.

(29) Hafner, F.; Holler, E.; von Angerer, E. Effect of growth factors on estrogen receptor mediated gene expression. *J. Steroid Biochem. Mol. Biol.* **1996**, *58*, 385−393.

(30) Biberger, C.; von Angerer, E. 1-Benzyl-2-phenylindole- and 1,2-diphenylindole-based antiestrogens. Estimation of agonist and antagonist activities in transfection assays. *J. Steroid. Biochem. Mol. Biol.* **1998**, *64*, 277−285.

(31) Brzozowski, A. M.; Pike, A. C. W.; Dauter, Z.; Hubbard, R. W.; Bonn, T.; Engström, O.; Öhman, L.; Greene, G. L.; Gustafsson, J.-Å.; Carlquist, M. Molecular basis of agonism and antagonism in the oestrogen receptor. *Nature* **1997**, *389*, 753−758.

(32) Tanenbaum, D. M.; Wang, Y.; Williams, S. P.; Sigler, P. B. Crystallographic comparison of the estrogen and progesterone receptor's ligand binding domains. *Proc. Natl. Acad. Sci. U.S.A.* **1998**, *95*, 5998−6003.

(33) Shiau, A. K.; Barstad, D.; Loria, P. M.; Cheng, L.; Kushner, P. J.; Agard, D. A.; Greene, G. L. The structural basis of estrogen receptor/coactivator recognition and the antagonism of this interaction by tamoxifen. *Cell* **1998**, *95*, 927−937.

(34) Jin, L.; Borras, M.; Lacroix, M.; Legros, N.; Leclercq, G. Antiestrogenic activity of two 11β-estradiol derivatives on MCF-7 breast cancer cells. *Steroids* **1995**, *60*, 512−518.

(35) Claussner, A.; Nedelec, L.; Nique, F.; Philibert, D.; Teutsch, G.; Van de Velde, P. 11β-amidoalkyl estradiols, a new series of pure antiestrogens. *J. Steroid Biochem. Mol. Biol.* **1992**, *41*, 609−614.

(36) Van de Velde, P.; Nique, F.; Planchon, P.; Prevost, G.; Bremaud, J.; Hameau, M. C.; Magnien, V.; Philibert, D.; Teutsch, G. RU 58668: further in vitro and in vivo pharmacological data related to its antitumoral activity. *J. Steroid Biochem. Mol. Biol.* **1996**, *59*, 449−457.

(37) Hanson, R. N.; Napolitano, E.; Fiaschi, R. Novel high-affinity steroidal estrogenic ligands: synthesis and receptor binding of 11β-vinyl-17 α-*E*/*Z*-phenylselenovinyl estradiols. *Steroids* **1998**, *63*, 479−483.

(38) Anstead, G. M.; Carlson, K. E.; Katzenellenbogen, J. A. The estradiol pharmacophore: ligand structure-estrogen receptor binding affinity relationships and a model for the receptor binding site. *Steroids* **1997**, *62*, 268−303.

(39) Poupaert, J. H.; Lambert, D. M.; Vamecq, J.; Abul-Hajj, Y. J. Molecular modeling studies on 11β-aminoethoxyphenyl and 7α-aminoethoxyphenyl estradiols. Evidence suggesting a common hydrophobic pocket in estrogen receptor. *Bioorg. Med. Chem. Lett.* **1995**, *5*, 839−842.

(40) Tedesco, R.; Katzenellenbogen, J. A.; Napolitano, E. 7α,11β-disubstituted estrogens: probes for the shape of the ligand binding pocket in the estrogen receptor. *Bioorg. Med. Chem. Lett.* **1997**, *7*, 2919−2924.

(41) Levenson, A. S.; Jordan, V. C. The key to the antiestrogenic mechanism of raloxifene is amino acid 351 (aspartate) in the estrogen receptor. *Cancer Res.* **1998**, *58*, 1872−1875.

(42) MacGregor Schafer, J.; Liu, H.; Bentrem, D. J.; Zapf, J. W.; Jordan, V. C. Allosteric silencing of activating function 1 in the 4-hydroxytamoxifen estrogen receptor complex is induced by substituting glycine for aspartate at amino acid 351. *Cancer Res.* **2000**, *60*, 5097−5105.

(43) Jordan, V. C.; MacGregor Schafer, J.; Levenson, A. S.; Liu, H.; Pease, K. M.; Simons, L. A.; Zapf, J. W. Molar classification of estrogens. *Cancer Res.* **2001**, *61*, 6619−6623.

(44) Bradford, M. M. A rapid and sensitive method for the quantification of microgram quantities of protein utilizing the principle of protein-dye binding. *Anal. Biochem.* **1976**, *72*, 248−254.

JM0208368